ELSEVIER

Biochimica et Biophysica Acta 1565 (2002) 246–266

BIOCHIMICA ET BIOPHYSICA ACTA
BBA

www.bba-direct.com

Review

Ca^{2+}-ATPase structure in the E1 and E2 conformations: mechanism, helix–helix and helix–lipid interactions

A.G. Lee*

Division of Biochemistry and Molecular Biology, School of Biological Sciences, University of Southampton, Bassett Crescent East, Southampton SO16 7PX, UK

Received 5 October 2001; received in revised form 22 May 2002; accepted 24 May 2002

Abstract

The determination of the crystal structure of the Ca^{2+}-ATPase of sarcoplasmic reticulum (SR) in its Ca^{2+}-bound [Nature 405 (2000) 647] and Ca^{2+}-free forms [Nature 418 (2002) 605] gives the opportunity for an analysis of conformational changes on the Ca^{2+}-ATPase and of helix–helix and helix–lipid interactions in the transmembrane (TM) region of the ATPase. The locations of the ends of the TM α-helices on the cytoplasmic side of the membrane are reasonably well defined by the location of Trp residues and by the location of Lys-262 that snorkels up to the surface. The locations of the lumenal ends of the helices are less clear. The position of Lys-972 on the lumenal side of helix M9 suggests that the hydrophobic thickness of the protein is only about 21 Å, rather than the normal 30 Å. The experimentally determined TM α-helices do not agree well with those predicted theoretically. Charged headgroups are required for strong interaction of lipids with the ATPase, consistent with the large number of charged residues located close to the lipid–water interface. Helix packing appears to be rather irregular. Packing of helices M8 and M10 is of the 3–4 ridges-into-grooves or knobs-into-holes types. Packing of helices M5 and M7 involves two Gly residues in M7 and one Gly residue in M5. Packing of the other helices generally involves just one or two residues on each helix at the crossing point. The irregular packing of the TM α-helices in the Ca^{2+}-ATPase, combined with the diffuse structure of the ATPase on the lumenal side of the membrane, is suggested to lead to a relative low activation energy for changing the packing of the TM α-helices, with changes in TM α-helical packing being important in the process of transfer of Ca^{2+} ions across the membrane. The inhibitor thapsigargin binds in a cleft between TM α-helices M3, M5 and M7. It is suggested that this and other similar clefts provide binding sites for a variety of hydrophobic molecules affecting the activity of the Ca^{2+}-ATPase.

Keywords: Sarcoplasmic reticulum; Ca^{2+}-ATPase; Lipid–protein interaction; Calcium pump; Helix packing; Membrane protein structure

1. Introduction: mechanism of the Ca^{2+}-ATPase

Intrinsic membrane proteins must have co-evolved with the lipid component of the membrane to give optimal function, within the constraints imposed by the role of lipids in the general physiology of the cell and by the requirements of the biosynthetic machinery for translation and insertion of proteins into membranes. The rules describing the relationships between protein structure and lipid structure are still being defined. The lipid compositions of biological membranes are complex and this complexity may be necessary for the proper function of membrane proteins. The lipid composition of the membrane affects properties of the membrane such as membrane thickness, the charge on the membrane, membrane phase (bilayer or gel) and intrinsic curvature (if it contains lipids such as the phosphatidylethanolamines that prefer a curved hexagonal HII phase rather than a planar bilayer phase). The importance of these various properties of a lipid bilayer have been studied for only a small number of membrane proteins that can be purified and reconstituted into lipid bilayers of defined composition. One such protein is the Ca^{2+}-ATPase from skeletal muscle sarcoplasmic reticulum (SR). The report of the crystal structure of the Ca^{2+}-ATPase of skeletal muscle SR in its Ca^{2+}-bound form [1] provides an opportunity to interpret these data in structural terms.

The ATPase contains 10 transmembrane (TM) α-helices and three large cytoplasmic domains (Fig. 1). The first of the

Abbreviations: TM, transmembrane; SR, sarcoplasmic reticulum; ER, endoplasmic reticulum; di(C14:1)PC, dimyristoleoylphosphatidylcholine; di(C18:1)PC; dioleoylphosphatidylcholine

* Tel.: +44-23-8059-4331; fax: +44-23-8059-4459.
E-mail address: agl@soton.ac.uk (A.G. Lee).

0005-2736/02/$ - see front matter © 2002 Elsevier Science B.V. All rights reserved.
PII: S0005-2736(02)00573-4

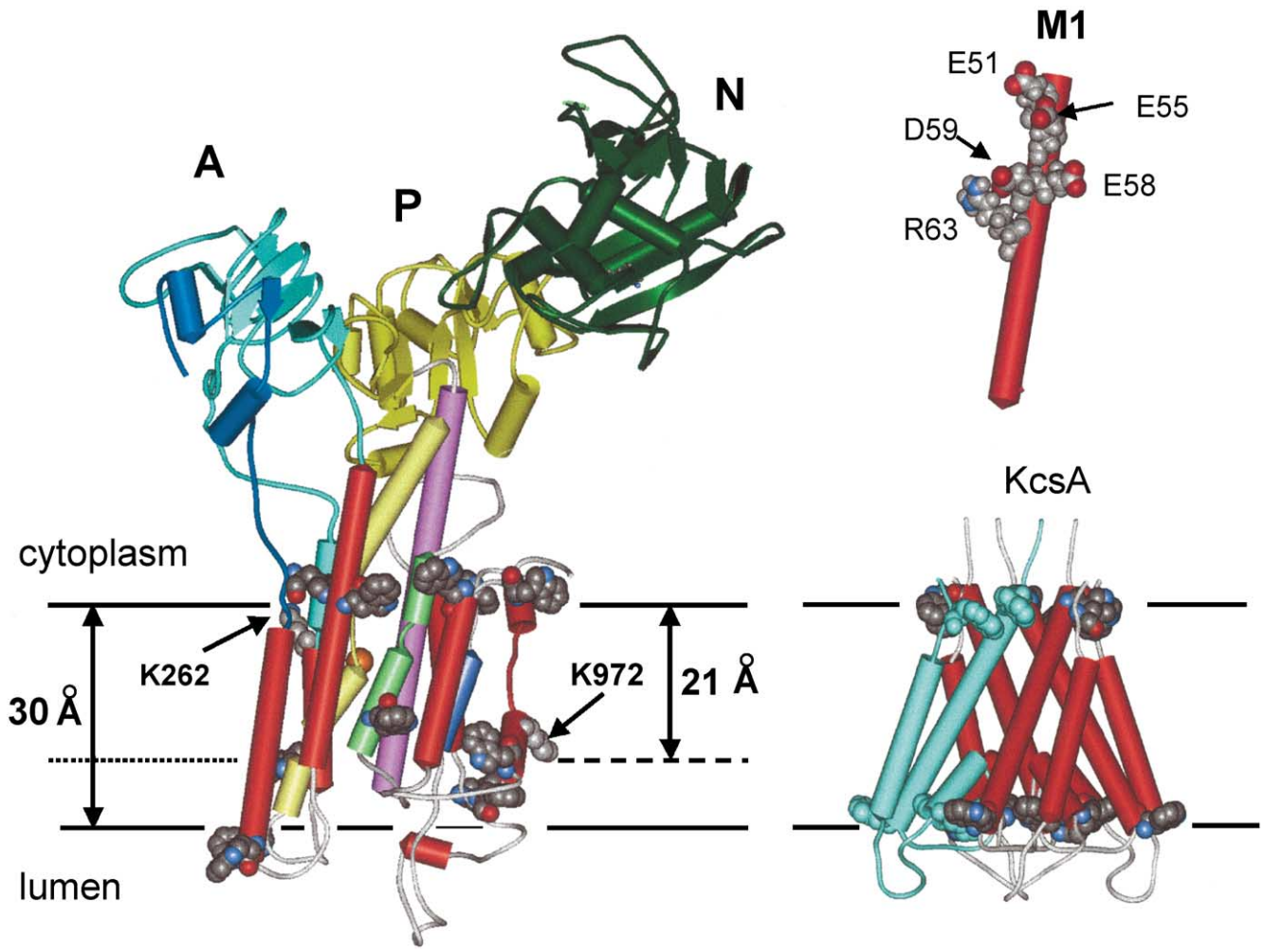

Fig. 1. The structure of the Ca^{2+}-ATPase in its Ca^{2+}-bound form. Shown are the structures of the Ca^{2+}-ATPase and of the potassium channel KcsA. The cytoplasmic domains of the Ca^{2+}-ATPase are coloured as follows: activation domain A, blue; phosphorylation domain P, yellow; nucleotide binding domain N, green. The four TM α-helices involved in binding Ca^{2+} ions are coloured as follows: M4, yellow; M5, lilac; M6, green; M8, blue; the other TM α-helices are coloured red. Only one of the two bound Ca^{2+} ions is visible in this view (shown in orange). The Trp residues close to the membrane are shown in space-fill representation. Also shown in space-fill representation are two Lys residues (K262 and K972) that help to define, respectively, the cytoplasmic and lumenal surfaces of the membrane. The horizontal lines show possible locations for the hydrocarbon core of bilayers of thickness 30 or 21 Å, as marked. The insert shows the structure of TM α-helix M1 with the charged residues shown in space-fill representation. KcsA is a tetramer in the membrane; one monomer is shown in blue and the other three in red. Trp residues are shown in space-fill representation.

cytoplasmic domains, initially referred to as the transduction or β-strand domain, is a 125-residue loop connected to TM α-helices M2 and M3 and is now referred to as the activation or A domain [1]. A larger loop of about 410 residues, connected to TM α-helices M4 and M5, makes up the phosphorylation domain P and contains the residue (Asp-351) phosphorylated by ATP. Inserted into the P domain is the nucleotide-binding domain N. Two Ca^{2+} ions are bound within the TM region, between helices M4, M5, M6 and M8. The two Ca^{2+} ions are bound side by side, 5.7 Å apart, at almost the same distance from the membrane surface. Site I contains oxygen ligands from M5, M6 and M8 whereas site II contains oxygen ligands predominantly from M4 (see Fig. 13). The two sites are bridged by Asp-800 in M6 that contributes carboxyl oxygen to both sites. Coordination at site I is provided by side chain oxygens of Asn-768 and Glu-771 from M5, Thr-799 and Asp-800 from M6, and Glu-908 from M8. Disruption of the helical structure of M6 around Asp-800 and Gly-801 is required to allow both Thr-799 and Asp-800 to contribute to the site [1]. Coordination at site II is provided by side chain oxygens of Asn-796 and Asp-800 from M6 and Glu-309 from M4 and by backbone oxygens of Val-304, Ala-305 and Ile-307 from M4. Again, this pattern of coordination requires that the helix mainly contributing ligands to the site (M4) be unwound between Ile-307 and Gly-310. The unwound region of M4 contains the PEGL motif found in the P-type ATPases, where Cys or His replaces the Glu residue in ATPases that transport heavy metals [2].

The pathway for transport across the membrane is very obvious in proteins such as the porins and in ion channels such as the potassium channel KcsA, but this is not the case

for the Ca^{2+}-ATPase (Fig. 1). There are no large channels leading from the cytoplasmic surface of the membrane to the pair of high affinity Ca^{2+} binding sites or leading from the binding sites to the lumenal surface of the membrane. This implies that significant conformational changes are required in the ATPase for transport, resulting in a rate of ion movement for the Ca^{2+}-ATPase that is very much lower than the rate of ion movement through an ion channel.

The mechanism of the Ca^{2+}-ATPase is usually discussed in terms of the E1–E2 model developed from the Post-Elbers scheme for (Na^+,K^+)-ATPase, as shown in Fig. 2 [3]. The model proposes that the Ca^{2+}-ATPase can exist in one of two distinct forms, E1 or E2. In the E1 conformation the ATPase can bind two Ca^{2+} ions from the cytoplasmic side of the membrane whereas in the E2 conformation these two sites are closed. Following binding of ATP, the ATPase is phosphorylated on Asp-351 to give a phosphorylated intermediate $E2PCa_2$, a state in which the two Ca^{2+} binding sites are of low affinity and face inwards. Following loss of Ca^{2+} to the lumen of the SR the ATPase dephosphorylates to E2 and then recycles to E1. The ATPase must also contain a pair of low affinity binding sites for Ca^{2+} on the lumenal side of the membrane to explain the effects of lumenal Ca^{2+} ions on the ATPase [4,5]. In the four-site model for transport by the Ca^{2+}-ATPase, transport of Ca^{2+} across the membrane corresponds to transfer of the two bound Ca^{2+} ions from the pair of cytoplasmic sites to the pair of lumenal sites on phosphorylation of the ATPase [4]. In this model, therefore, the two bound Ca^{2+} ions are released from a different pair of sites (the lumenal pair of sites) to those to which they initially bound (the cytoplasmic pair of sites). As described elsewhere [5], mutagenic and structural data do not fit easily with this form of the four-site model; the experimental data are more easily interpreted in terms of the alternating, four-site model for transport shown in Fig. 2. In this model the transported Ca^{2+} ions are released directly from the cytoplasmic pair of sites, linked to closure of a pair of lumenal binding sites [5]. Thus, in the alternating four-site model the pair of lumenal Ca^{2+} binding sites is available to bind Ca^{2+} in the E1 and E2 conformations of the ATPase but not in the phosphorylated form $E2PCa_2$,, as shown in Fig. 2, and the pair of transport sites is open to the lumen in the phosphorylated intermediate $E2PCa_2$ but is closed to the lumen in the non-phosphorylated states E1 and E2.

An unexpected feature of the structure of the Ca^{2+}-ATPase is that the first TM α-helix (M1) contains four acidic and one basic residue (Fig. 1). Since one of the acidic residues (Glu-58) points towards the Ca^{2+} ion in binding site II, it has been suggested that helix M1 could be part of the access pathway to Ca^{2+} binding site II, with a Ca^{2+} ion reaching site I through site II, explaining the cooperativity in Ca^{2+} binding and the observation that binding of the second Ca^{2+} ion blocks the release of the first Ca^{2+} ion to bind [5]. Since there is no obvious pathway from the high affinity sites to the lumenal surface of the membrane, release of Ca^{2+} ions from the ATPase must involve a significant change in the packing of the TM α-helices. This could involve an opening up of the interface between helical bundles M1–M4 and M5–M10, allowing access to the lumen [5].

The link between the phosphorylation domain and the pair of high affinity Ca^{2+} binding sites is probably provided by two small helices P1 and P2 in the phosphorylation domain that contact the loop between TM α-helices M6 and

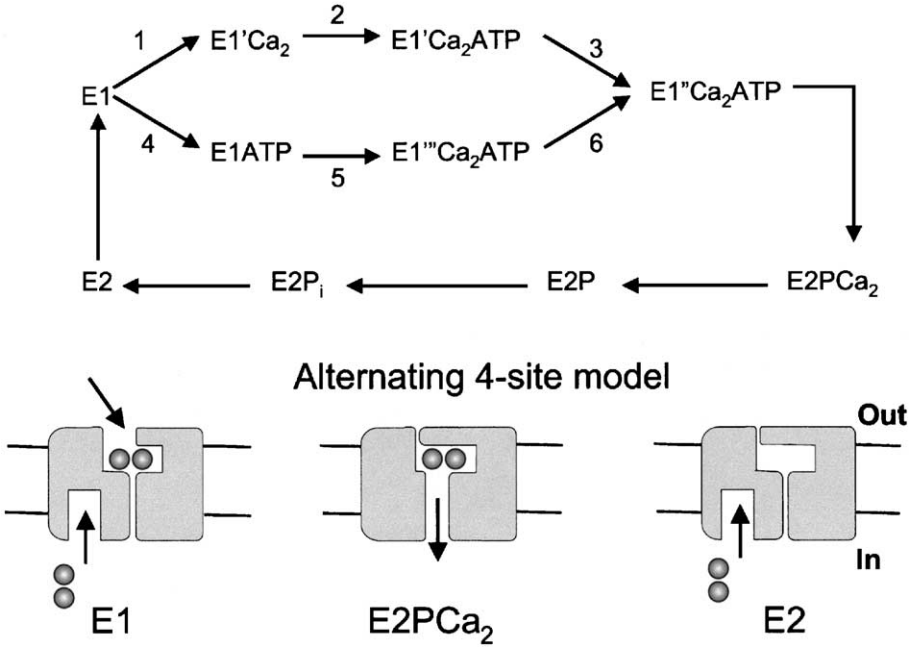

Fig. 2. The E1–E2 scheme for the Ca^{2+}-ATPase. Also shown is a representation of the alternating four-site model for transport, showing the proposed changes in the cytoplasmic and lumenal binding sites for Ca^{2+} [5].

M7 (see Fig. 12) [1]. P1 is close to Asp-351, the residue phosphorylated by ATP. Since there are large changes in the conformation of the ATPase on binding ATP and phosphorylation [1] it is likely that P1 moves on phosphorylation of the ATPase. Movement of P1 relative to the M6–M7 loop on phosphorylation could move the M6–M7 loop, and so lead to a change in the packing of the TM α-helices, leading to conversion of the pair of cytoplasmic binding sites for Ca^{2+} from a state of high affinity for Ca^{2+} to one of low affinity, followed by release of the two bound Ca^{2+} ions. Conversely, binding of Ca^{2+} to the pair of cytoplasmic sites on the Ca^{2+}-ATPase will change the packing of the TM α-helices, alter the position of the M6–M7 loop and thus alter the position of P1, signalling to the phosphorylation domain of the ATPase that Ca^{2+} is bound; only the Ca^{2+}-bound form of the ATPase can be phosphorylated by ATP. Thus, the pattern of packing of the TM α-helices of the Ca^{2+}-ATPase and changes in this pattern of packing on binding Ca^{2+} and on phosphorylation are key to the function of the ATPase. This idea is explored further in Section 5 where the structure of the Ca^{2+}-bound ATPase is compared to that of the Ca^{2+}-free, E2 form. Since the TM α-helices are embedded in the lipid bilayer, it is not surprising that changes in the structure of the lipid bilayer lead to changes in the function of the ATPase [6].

2. Identification of TM α-helices

The crystal structure of the Ca^{2+}-ATPase contains no resolved phospholipid molecules so that it is not possible to identify directly from the crystal structure which regions of the Ca^{2+}-ATPase actually span the lipid bilayer. TM α-helices are usually predicted on the basis of hydropathy plots, searching for long stretches of hydrophobic amino acid residues. This definition of a TM α-helix equates the TM region to the part of a helix required to span the hydrocarbon core (the fatty acyl chain region) of a lipid bilayer, which, for a typical phospholipid bilayer such as dioleoylphosphatidylcholine (di(C18:1)PC), has a thickness of about 30 Å. Given a helix translation of 1.5 Å/residue in a perfect α-helix, about 20 residues are required to span the hydrocarbon core of the bilayer if the helix is untilted with respect to the bilayer normal; a tilt of about 20°, typical of that found in many membrane proteins, would increase this by about 10%. However, a requirement to cap the ends of α-helices may extend the length of the helix. The requirement for capping follows because the initial four –NH and final four –C=O groups of an α-helix have no hydrogen bonding partners provided by the peptide backbone of the α-helix itself, and so suitable hydrogen bonding partners have to be provided in some other way. One way is to extend the helix by three or four residues at each end with polar residues containing suitable hydrogen bonding partners such as Pro and Asn. For example, in the Ca^{2+}-ATPase Asn-810 and Asn-930 at the cytoplasmic ends of M6 and M9, respectively, and Asn-275, Pro-789 and Pro-952 at the lumenal ends of M3, M6 and M9, respectively, will serve this role. Alternatively, if hydrophobic, nonpolar residues in the TM α-helix extend into the headgroup region, hydrogen bonds could form with suitable groups in the glycerol backbone and headgroup regions of the lipid bilayer. The result is that there is a degree of uncertainty in where the ends of TM α-helices should be drawn. In the same way that the lipid–water interface is not a sharp boundary [7], so there is a degree of indeterminacy in locating the ends of TM α-helices. If 20 residues are required to span the hydrophobic core of the bilayer, the total helix length could be up to 28 residues. For example, the average number of residues in the TM α-helices of the bacterial photoreaction centre is 26, corresponding to a length of about 39 Å. The hydrophobic stretches in these helices are, however, about 19 amino acids or about 28.5-Å long [8,9]. This corresponds closely to the hydrophobic thickness of about 30 Å, defined experimentally as that part covered by detergent in the crystal [10,11].

Identification of the ends of TM α-helices is made easier by the fact that Trp and Tyr residues are often found at the ends of TM α-helices. This observed preference for Trp and Tyr residues for the ends of TM α-helices agrees with measurements of the binding of small peptides at the lipid–water interface that show that aromatic residues have a preference for the lipid–water interface [12]. Further, a number of small tryptophan analogues have been shown to bind in the glycerol backbone and lipid headgroup region of a lipid bilayer, stabilised partly by location of the aromatic ring in the electrostatically complex environment provided by this region of the bilayer, and partly by exclusion of the flat, rigid ring system from the hydrocarbon core of the bilayer for entropic reasons [13]. The aromatic residues at the ends of TM α-helices probably act as 'floats' at the interface, serving to fix the helix within the lipid bilayer. However, it is at present unclear whether the aromatic rings prefer the hydrocarbon or the headgroup region of the bilayer. This uncertainty is also apparent in the crystal structures of a number of membrane proteins. For example, the Trp residues in the bacterial potassium channel KcsA [14] are found clustered at the ends of the TM α-helices, forming clear bands on the two sides of the membrane, as shown in Fig. 1. Assuming a hydrophobic thickness for the membrane of 30 Å, the Trp residues in KcsA would be located just below the glycerol backbone region of the bilayer, at the outer edges of the hydrocarbon core. In the bacterial photosynthetic reaction centre [15], the majority of the Trp residues are found near the periplasmic side of the protein, again near the ends of the TM α-helices. However, the band of Trp residues is more diffuse than in KcsA and if the hydrocarbon core of the bilayer around the complex has a thickness of 30 Å, then some Trp residues will be located in the hydrocarbon core and some will be in the headgroup regions of the bilayer. Consistent with this

interpretation, detergent molecules in the crystal structure are seen to cover some of the Trp residues on the periplasmic and cytoplasmic sides of the membrane, but not others [11].

Defining the beginning and ends of the TM regions of the TM α-helices is particularly difficult for the Ca^{2+}-ATPase (Fig. 1). Many of the TM α-helices extend above the membrane surface to form a central stalk linking the TM region to the cytoplasmic head of the protein. As a consequence, some of the helices are very long; helix M5 for example contains 41 residues. Nevertheless, the probable location of the cytoplasmic surface of the ATPase is relatively well defined by the ring of Trp residues on this side of the ATPase (Fig. 1). A Lys residue (Lys-262) in TM α-helix M3 can be seen pointing up from the hydrophobic core of the bilayer like a snorkel. Since the cost of burying a charged residue in the hydrophobic core of a bilayer is very high (about 37 kJ mol^{-1} for a Lys residue; [16]), it is likely that the amino group on Lys-262 will be located at the hydrophobic interface; the Trp residues in the Ca^{2+}-ATPase will then be located in the headgroup region of the bilayer, as shown in Fig. 1.

The distribution of Trp residues on the lumenal face of the Ca^{2+}-ATPase is much more diffuse than on the cytoplasmic side (Fig. 1). The hydrophobic thickness of the Ca^{2+}-ATPase could be expected to be about 30 Å since this is the hydrophobic thickness of a bilayer of di(C18:1)PC, the phospholipid that supports highest activity for the ATPase [17]. However, as shown in Fig. 1, this definition locates a Lys residue in M10 (Lys-972) totally within the hydrocarbon core, which seems unlikely. The hydrophobic thickness of the bilayer would have to be about 21 Å to locate the two interhelical loops and Lys-972 at the lumenal surface (Fig. 1). However, this is unusually thin for a membrane protein and is close to the thickness of a bilayer of dimyristoleoylphosphatidylcholine (di(C14:1)PC), which is 22 Å.

Although the hydrophobic thickness of the Ca^{2+}-bound ATPase appears to match best a bilayer of di(C14:1)PC, the conformation of the ATPase actually adopted in a bilayer of di(C14:1)PC is an abnormal one. For example, the ATPase in di(C14:1)PC binds only a single Ca^{2+} ion instead of the normal two and the activity of the Ca^{2+}-ATPase in di(C14:1)PC is much less than that in di(C18:1)PC [18,19]. The abnormal E1 conformation adopted in di(C14:1)PC could result from the requirement to tilt the longer helices to match the thin di(C14:1)PC bilayer; although a thin bilayer would be favourable for helix M10 because of the favourable location of Lys-972, it would be less favourable for the longer helices such as M1 that would have to tilt to locate all their hydrophobic residues within the hydrophobic core of a thin bilayer. Alternatively, the structure of the Ca^{2+}-ATPase crystallised from the detergent $C_{12}E_8$ and shown in Fig. 1 could be slightly different to that in a bilayer of a normal lipid such as di(C18:1)PC, particularly with respect to the organization of the helices on the lumenal side of the membrane. If the structure of the Ca^{2+}-ATPase in a bilayer of di(C18:1)PC is the same as that shown in Fig. 1, then it would seem to require some thinning of the bilayer around the ATPase, implying that the Ca^{2+}-ATPase would exist in a state of stress within the native membrane.

Assuming a hydrophobic thickness of 21 Å for the TM α-helices in the Ca^{2+}-bound form defines the TM regions of the TM α-helices as shown in Fig. 3. Helices M1, M2, M3, M4, M7 and M8 extend beyond the lumenal ends of the boundaries defined in this way. Assuming a hydrophobic thickness of 30 Å for the ATPase gives the longer TM regions defined in Fig. 3. The definition of the TM helices shown in Fig. 3 gives a length for the TM region of the

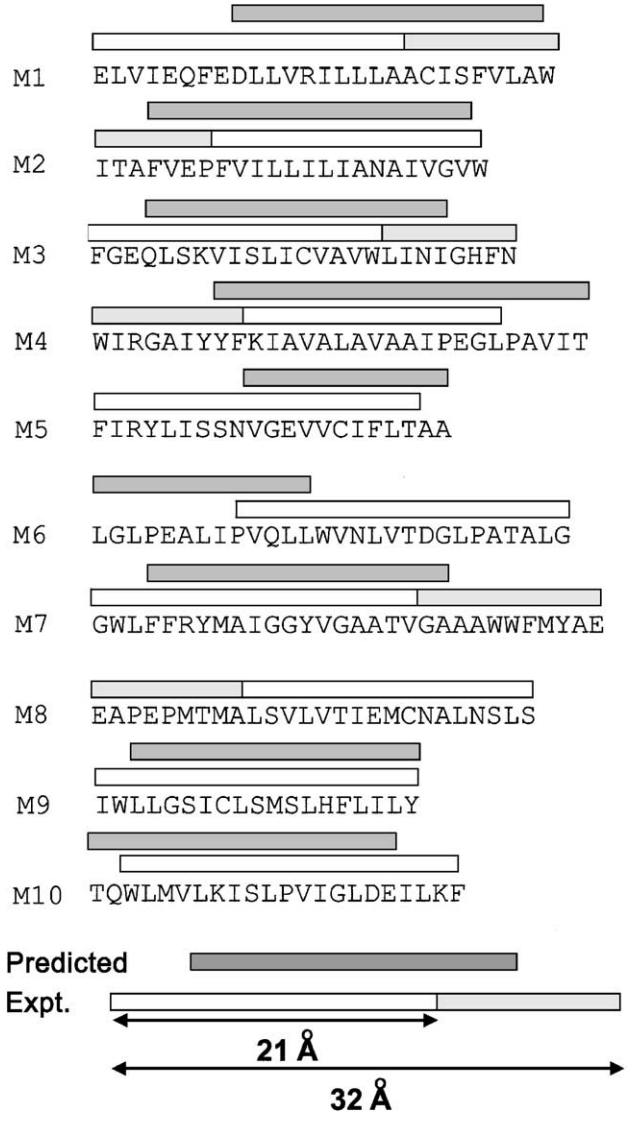

Fig. 3. Possible definitions for the TM regions of the TM α-helices of the Ca^{2+}-ATPase in its Ca^{2+}-bound form. Assuming a hydrophobic thickness for the ATPase of 21 Å in the E1 conformation gives the sequences defined by the open bars. If the hydrophobic thickness is 30 Å then helices M1, M2, M3, M4, M7 and M8 are extended on the lumenal side as shown by the lightly shaded bar. Also shown by the upper darkly shaded bar are the TM α-helices predicted using the PredictProtein programme.

helices of between 15 and 20 residues with an average number of residues of 18.4 if the hydrophobic thickness of the ATPase is 21 Å. If the hydrophobic thickness of the ATPase is 30 Å then the average length of the TM α-helices would be 28.2.

Leu is the most common residue in the TM α-helices of the Ca^{2+}-ATPase, as it is in many other membrane proteins [20,21], making up 19.8% of the residues, but the helices are also relatively rich in the bulky residues Ile (11.5%) and Val (12.1%); Ala makes up just 9.3%. Thus, factors such as residue volume and packing, which are important in determining helix stability in water soluble proteins, are not so important for TM α-helices; effects of large residue volume will, in the membrane, be balanced by the favourable hydrophobic interactions of a large side chain with the fatty acyl chains. In water-soluble proteins, the conformationally flexible Gly residue is also classed as a helix breaker since it is an intrinsically flexible residue with the potential to adopt most of the dihedral angles available in a Ramachandran plot. Gly is quite common in the TM α-helices of the Ca^{2+}-ATPase (6.5%), suggesting that its potential flexibility is constrained in the bilayer environment. As Gly possesses the smallest of all the side chains, it may play a role in mediating helix–helix interactions and packing in the membrane, as described later. The polar amino acid most commonly found within the TM α-helices is Ser (6.0%) with small amounts of Cys (2.2%) and Thr (2.7%). Of the aromatic residues, Trp makes up 3.3%, Tyr, 2.2% and Phe 4.9%. Acidic residues Asp (1.6%) and Glu (6.5%) are more common in the Ca^{2+}-ATPase than in the TM α-helices of other membrane proteins, obviously related to their function in binding Ca^{2+}. There are also three Lys residues, one His residue, five Asn residues and three Gln residues.

The TM α-helices as defined in Fig. 3 can be compared to the results of prediction programmes such as the PredictProtein programme available on http://www.emblheidelberg.de/Services/index.html. The TM α-helices predicted for the Ca^{2+}-ATPase are shown in Fig. 3, and serve to illustrate the problems in identifying TM α-helices for complex, multi-spanning membrane proteins. First, PredictProtein predicts nine TM α-helices whereas the X-ray crystal structure shows that there are ten—M8 is not predicted. Second, whereas the sequences of some TM α-helices agree well with experiment, for others the agreement is rather poor. In part this is due to the difficulty in defining the start and end points for TM α-helices in the crystal structure as already described. Not surprisingly, agreement between prediction and experiment is weakest when the TM α-helices contain charged residues as, for example, in the first TM α-helix that contains four acidic residues at the N-terminal end. Better agreement between predicted TM α-helices and experiment is obtained when predictions are based on comparisons between members of the Ca^{2+}-ATPase family [64].

3. The lipid-exposed surface of the Ca^{2+}-ATPase

In general, residues in contact with lipids are less well conserved than those that point to the interior of a protein and, in families of related membrane proteins, lipid-facing residues have substitution patterns distinctly different to those for buried residues in water soluble proteins [22–24]. This is consistent with the idea that interactions between hydrophobic amino acid side chains and lipid fatty acyl chains are relatively undemanding structurally whereas residues involved in protein–protein contact would be expected to be more highly conserved. The vast majority of the residues on the Ca^{2+}-ATPase exposed to the lipid fatty acyl chains are hydrophobic. An exception is the pair of charged residues Asp-59 and Arg-63 in M1 that are exposed to the lipid fatty acyl chains in the Ca^{2+}-bound form. However, Asp-59 is stacked against Arg-63 and so presumably forms a salt bridge with it (Fig. 1). This unusual feature is conserved in the ER/SR class of Ca^{2+}-ATPase and could be important in maintaining the correct conformation for helix M1. In helix M3, Lys-262 snorkels up to the cytoplasmic surface and Lys-972 snorkels down to the lumenal surface in M10. All other residues are hydrophobic.

The hydrophobic surface of the ATPase is molecularly rough, as shown in Fig. 4, which also shows how parts of the surface overhang the lipid bilayer. Clearly, most phospholipids will not be bound at distinct ‘sites’ around the ATPase but rather should be pictured as interacting with the hydrophobic surface of the ATPase. The interaction between lipids and this surface is short-lived, as shown by the rapid rate of lipid exchange on and off the protein [25]. A charged headgroup is required for strong binding: oleic acid and oleylamine bind relatively strongly at the lipid–protein interface, but oleyl alcohol and methyl oleate bind very weakly [26], consistent with the presence of a wide range of charged groups in the regions either side of the hydrophobic surface. Binding of gel phase lipid is a factor of 20 weaker than binding of lipids in the liquid crystalline phase [17], presumably as a result of poor van der Waals contact between rigid chains and the rough protein surface. Weak binding of cholesterol at the lipid–protein interface [27] follows both from the lack of a charged headgroup and from the effect of the rigid ring system; cholesterol hemisuccinate with its negatively charged ‘headgroup’ binds more strongly than cholesterol [28] and a phosphatidylcholine in which one fatty acyl chain has been replaced by the cholesterol moiety, although it binds less well than a normal phosphatidylcholine, does so only by a factor of about 2 [29].

Importantly, the strength of binding of phospholipids to the Ca^{2+}-ATPase does not change significantly with chain length, the binding constants being the same for phosphatidylcholines with chain lengths between C14 and C24 [17,30]. Since the cost of exposure of hydrophobic groups to water (either the lipid chains or the protein) is high, it has often been suggested that lipids will distort to match the hydrophobic thickness of the protein. Stretching or com-

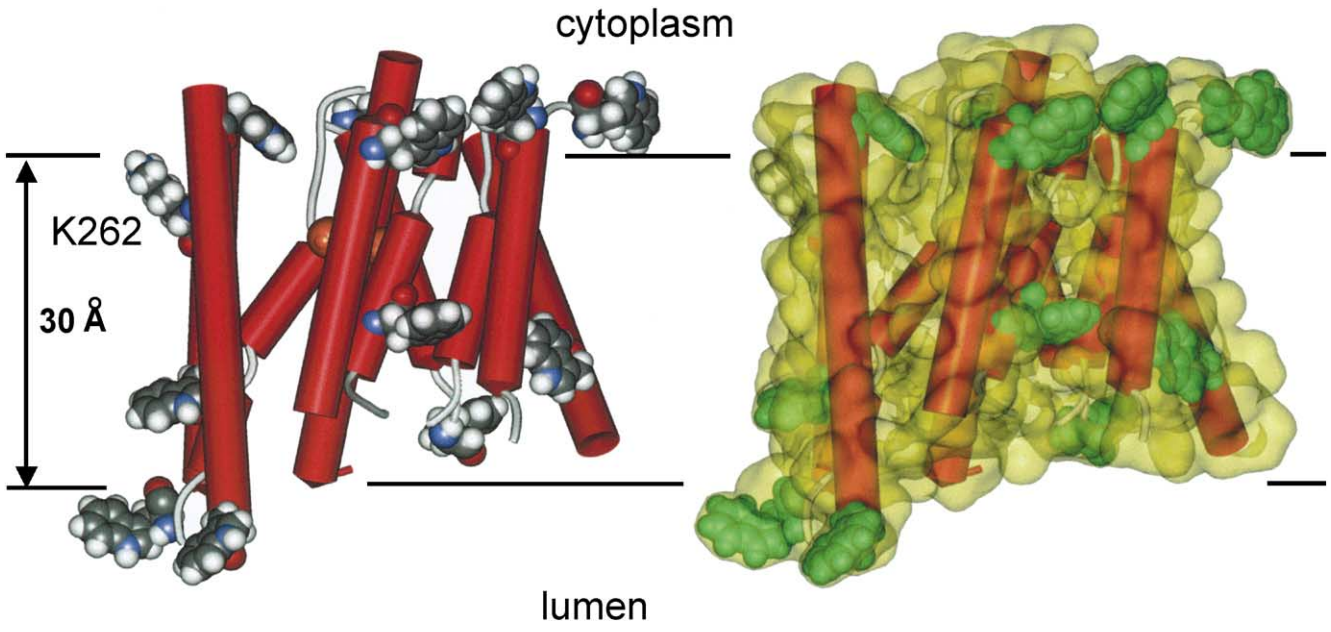

Fig. 4. A view of the TM α-helices of the Ca^{2+}-ATPase in its Ca^{2+}-bound form and the corresponding molecular surface.

pressing the lipid bilayer will, however, have an energetic cost that would be expected to be matched by changes in lipid binding constant with chain length. Since this is not seen, it seems that the ATPase must, in fact, distort to match the thickness of the lipid bilayer rather than the lipid bilayer distorting to match the thickness of the protein. These changes presumably correspond to changes in the tilt and in the packing of the TM α-helices, these, in turn, leading to the observed changes in ATPase activity with changing bilayer thickness. Tilting of TM α-helices has been suggested for synthetic, model TM α-helices [31,32]. If helices in the Ca^{2+}-ATPase do tilt rather easily to match the thickness of the surrounding lipid bilayer, then the organization of the helices, particularly helix M10, might be different in a bilayer of di(C18:1)PC from that in the Ca^{2+}-ATPase crystallized from the detergent $C_{12}E_8$, as suggested above.

The circumference of the hydrophobic surface of the Ca^{2+}-ATPase is about 140 Å. Assuming that a lipid in the liquid crystalline bilayer occupies a surface area of 70 $Å^2$, the effective diameter of a lipid molecule is 9.4 Å, so that about 30 lipid molecules will be required to form a bilayer shell around the ATPase. The number of lipid molecules forming an annular shell around the Ca^{2+}-ATPase has been estimated from ESR experiments to be 32 at low temperatures, although the figure drops to 22 at higher temperatures, possibly because of errors in the simulations at higher temperatures where exchange of lipid on and off the protein affects the spectra [25]. ESR spectra of spin-labelled lipid in Ca^{2+}-ATPase-containing membranes show the presence of two components, a mobile component from spin-label lipid in bulk lipid bilayer and an 'immobile' component due to lipid on the hydrophobic surface of the protein. The lipid in contact with the surface of the ATPase appears 'immobile' because it is spatially disordered and has reduced molecular motion because of its contact with the molecularly rough surface of the protein [25].

The minimum number of phospholipid molecules required to maintain the activity of the Ca^{2+}-ATPase is about 30 per ATPase molecule [25] corresponding closely to the number estimated above from the size of the TM α-helical bundle. There has been much discussion in the literature about the extent to which the annular shells of lipid around membrane proteins can be shared between membrane proteins. The observation that the minimum number of lipids required to maintain activity for the Ca^{2+}-ATPase is equal to the number required to cover the surface of its TM α-helical bundle suggests that the extent of sharing of annular lipid shells is very limited, even at low molar ratios of phospholipid to ATPase. This is, of course, consistent with the bulky nature of the cytoplasmic domains of the Ca^{2+}-ATPase, which will prevent extensive close contact between the TM α-helical regions of the ATPase.

As well as the phospholipid molecules interacting with the hydrophobic surface of the ATPase, evidence has been presented for the presence of sites (non-annular sites) to which a variety of hydrophobic molecules can bind but from which phospholipids are excluded. Molecules binding to such non-annular sites include cholesterol and simple alkanes [27,29,33]. The location of these sites on the ATPase is not obvious from the crystal structure but the molecular roughness of the surface might provide sites too small to bind phospholipids but able to bind smaller hydrophobic molecules, including sites between TM α-helices. A binding site of this type exists for thapsigargin, a hydrophobic inhibitor of the Ca^{2+}-ATPase (Section 5).

Phospholamban, a small membrane protein with a single TM α-helix, has been shown to interact with residues in the

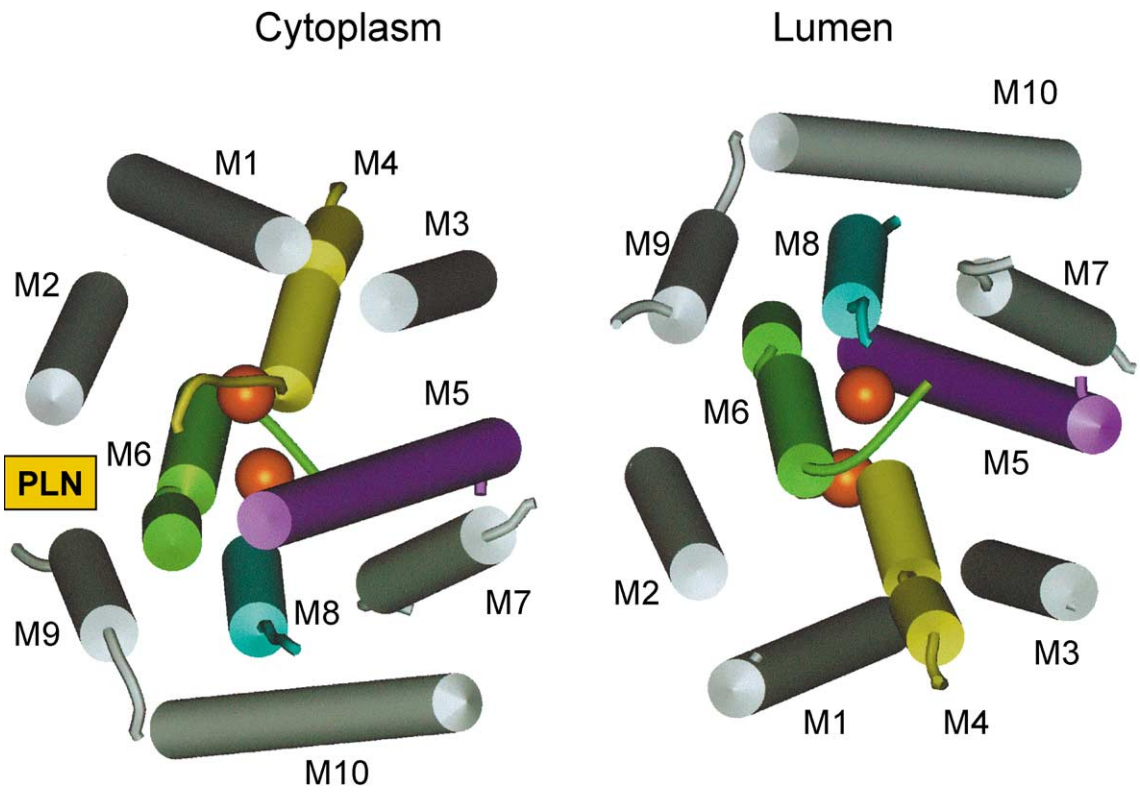

Fig. 5. The TM α-helices of the Ca^{2+}-ATPase in its Ca^{2+}-bound form, viewed from the cytoplasmic and lumenal sides of the membrane. The likely binding site for the transmembrane domain of phospholamban (PLN) is indicated. The two bound Ca^{2+} ions are shown in orange.

region ^{397}KNDKPV^{402} of skeletal muscle Ca^{2+}-ATPase [34]. These residues are located on the underside of the N domain in a region shown in antibody binding experiments to be exposed [35]. This region stretches from 29 to 40 Å above the bilayer surface. The cytoplasmic domain of phospholamban contains about 30 residues and so is able to reach up to this region of the ATPase. The TM domain of phospholamban interacts with helix M6 in the Ca^{2+}-ATPase and mutation of Leu-802 and Thr-805 on the lipid-exposed face of M6 disrupts interaction [36]. M6 lies at the base of a cleft bounded by M2 and M9 (Fig. 5). M9 contains two polar residues, Ser-936 and Ser-940, close to Leu-802 and Thr-805 in M6 that could be involved in hydrogen-bonding interactions with the TM domain of phospholamban.

4. Packing of TM α-helices

There is now much evidence that specific interactions between TM α-helices are important factors in determining the folding of integral membrane proteins. Popot et al. [37] have described multi-spanning membrane proteins as 'collegial' structures, built up of prefolded units. Each TM α-helix firsts folds as a unit, independent of the rest of the protein, which then packs with the other helices. This can be illustrated by experiments in which a bacteriorhodopsin molecule is regenerated from fragments. Chymotrypsin cleaves bacteriorhodopsin between helices B and C, giving fragments containing two and five TM α-helices. These, if refolded separately into lipid-detergent micelles and mixed, will regenerate bacterio-opsin (the protein without the retinal chromophore) [38]. Alternatively, the two fragments can be incorporated into lipid vesicles, where circular dichroism shows that each fragment contains the expected number of α-helices: if the vesicles are then fused, the fragments regenerate bacterio-opsin and, on addition of retinal, bacteriorhodopsin [39]. Neutron diffraction studies confirm that the packing of the TM α-helices in the regenerated bacteriorhodopsin is indistinguishable from that in the native bacteriorhodopsin molecule [40]. Again, synthetic peptides corresponding to the TM α-helices A and B of bacteriorhodopsin combined with the five TM α-helix chymotryptic fragment will also regenerate bacteriorhodopsin [41]. Even more surprising, it is possible to regenerate the seven-helix bundle by combining fragments even when there are redundant helices, for example by mixing a fragment containing TM α-helices A to E with one containing TM α-helices C to G [42]. These experiments show that the helices of bacteriorhodopsin contain all the information necessary to pack properly in the membrane. The individual TM α-helices can, in this sense, be considered as separate folding entities, whose packing is determined by the properties of the helices themselves. These experiments also show that the loops between the TM helices are not required for

the correct assembly of bacteriorhodopsin, although the loops do contribute to the stability of the molecule; assembled fragments are more susceptible to denaturation than is the native protein [42].

It has been estimated that 97% of TM α-helices next to each other in the sequence of a membrane protein are next to each other in the three-dimensional structure [43]. Next helices in the sequence of the Ca^{2+}-ATPase are next to each other in the three-dimensional structure of the ATPase, except for the two helices M3 and M6 (Fig. 5). Thus, M1 and M2 are nearest neighbours as are M3 and M4, and these pairs are linked by short lumenal loops of about eight residues, which would be consistent with their insertion into the membrane as helical hairpins. The relatively long loop between M2 and M3 (148 residues) would allow a relocation of the M1/M2 pair relative to the M3/M4 pair to put M1 close to M4. Similarly, in the pairs M5/M6, M7/M8 and M9/M10 next nearest helices in the sequence are nearest helices in the structure but M6 is out of position relative to M7, even though the cytoplasmic loop between M6 and M7 is relatively short (23 residues). This is interesting since the M6–M7 loop plays a special part in linking phosphorylation of the ATPase to the movements of the TM helices, as already described.

In the known crystal structures for membrane proteins, polar interactions between TM α-helices are rare. For example, in the photosynthetic reaction centre the only polar interactions involving the TM α-helices are those of the four His residues coordinating the heme iron; apart from these special interactions there are no salt bridges between TM α-helices and very few hydrogen bonds between helices [44]. This is also true for the Ca^{2+}-ATPase where there is only one direct salt bridge between helices, a salt bridge on the lumenal side of the membrane between Glu-90 in M2 and Lys-297 in M4; this salt bridge is also present in the Ca^{2+}-free form of the ATPase. Clearly the packing of helices M4, M5, M6 and M8 will be unusual because of the presence of acidic residues involved in binding the two Ca^{2+} ions to be transported. Packing of the other helices would, however, be expected to conform to the general rules for helical packing in membrane proteins.

The majority of interactions between helices in the Ca^{2+}-ATPase are between nonpolar residues, and thus van der Waals interactions must be central to interhelical packing. Relatively weak side-by-side interactions could be enough to stabilise a specific pattern of packing, particularly if the ends of the TM α-helices are constrained by short interconnecting extramembranous loops to be close together. Possible modes of packing of α-helices have been explored in detail for globular proteins. If α-helices were smooth cylinders then the most favourable mode of packing would be with their long axes packed either parallel or antiparallel. However, the surfaces of helices are not smooth. For a regular α-helix, amino acid side chains making up the surface of the α-helix will form a helical row around the surface, forming sets of parallel ridges separated by shallow furrows or grooves, as shown in Fig. 6 [45,46]. One set of ridges and grooves is formed by the following sets of residues: (4, 8 and 12); (7, 11, 15 and 19); (18 and 22), and so on. In this set, four residues separate the residues forming the ridges. Another set of ridges and grooves is formed by the following sets of residues: (4 and 7); (8 and 11); (12, 15 and 18); (19 and 22), and so on. One mode of helical packing is the packing of the ridges on one helix into the grooves of the other helix, and vice versa. A form of this mode of packing commonly found in globular proteins is where the ridges formed by side chains four residues apart pack with the corresponding grooves in the second helix. This pattern of packing, referred to as 4–4 packing, is illustrated in Fig. 6. The ridges and grooves form an angle of about 25° to the helical axis so that packing of ridges on one helix into grooves on the other helix requires that the two helices be oriented with their long axes making a right-handed crossing angle of −50° (25°+25°). Another common mode of packing is with the ridges formed by residues four apart fitting into the grooves formed by residues three apart, and vice versa, this being referred to as 3–4 packing. Residues three apart form ridges and grooves making an angle of 45° with the helical axis, oriented in the opposite direction to those formed by residues four apart (Fig. 6). In this case, packing of ridges into grooves requires a left-handed crossing angle between the helices of +20° (45°−25°).

An alternative to the ridges into grooves description of helix packing has been termed ‘knobs-into-holes’ packing and emphasises the idea that, to avoid unfavourable gaps at the interface between two helices, side chains in one helix (knobs) should pack into the spaces between the side chains (the holes) in the other [47]. As shown in Fig. 6, knobs-into-holes packing gives rise to a crossing angle of about 20°, the same as that in the 3–4 mode of ridges into grooves packing. However, knobs-into-holes and ridges into grooves packing differ in a small vertical offset between the two helices, so that in ridges into grooves packing, a residue from one helix is located between two others on the neighbouring helix whereas in knobs-into-holes packing side chains from one helix (knobs) pack into spaces between four other residues (holes) on the other helix. The differences between the two models are rather small but for many real proteins where the ridges and grooves are very irregular and difficult to identify, the knobs-into-holes model is a rather easier description to apply. In general it has been found that, whereas ridges into grooves packing describes the packing between short α-helical segments in globular proteins, packing between longer α-helices matches better the knobs-into-holes model [45].

Knobs-into-holes packing has been found to be particularly useful in describing packing in coiled-coil proteins. Coiled-coil proteins contain long α-helices with the α-helices maintaining close contact over most of their length. Classic examples of coiled-coil proteins include fibrous proteins such as tropomyosin, and transcription factors such as the yeast transcriptional activator GCN4. In a coiled-coil

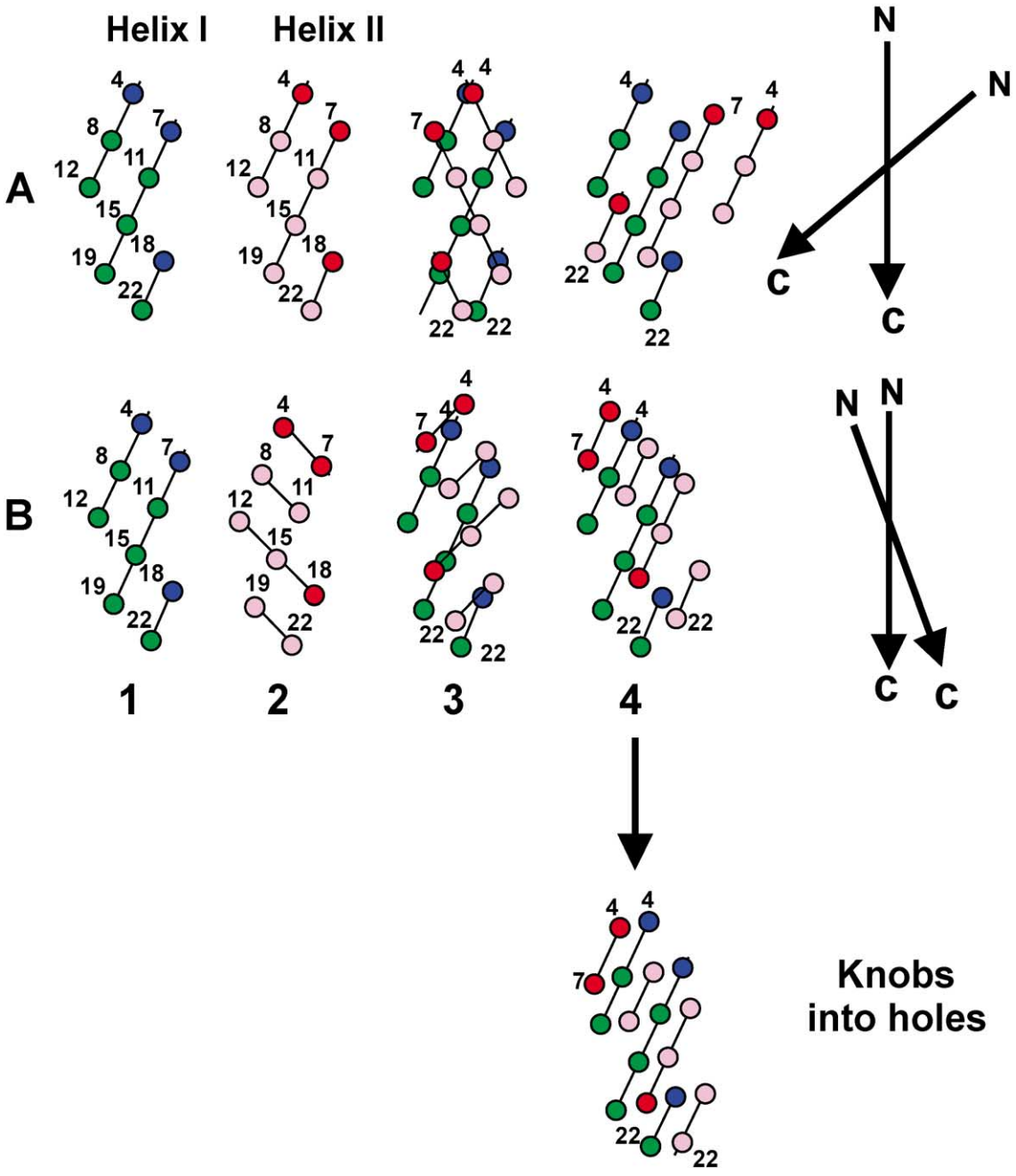

Fig. 6. Ridges and grooves and knobs-into-holes packing of α-helices. (A) 1 and 2 show two helices with the ridges formed by side chains four residues apart; residues in helix I are shown as blue and green circles and those in helix II as red and pink circles. To pack the helices against each other, helix II has been turned by 180° out of the plane of the paper and placed on top of helix I, as shown in 3 and then, in 4, the orientation of helix II is shifted by 50° to pack the ridges of helix II into the grooves of helix I and vice versa. This results in a packing of the two helices with an angle of 50° between their long axes. (B) 1 shows the ridges formed by side chains four residues apart whereas 2 shows the ridges formed by side chains three residues apart. In 3, helix II has been placed on top of helix I, as in (A). In this case, rotation of helix II by 20° in the direction opposite to that in (A) results in packing of ridges into groves. Knobs-into-holes packing results when the two helices are offset slightly vertically from each other, as shown in the bottom figure.

protein there may be two, three or four α-helices in a bundle, with the helices either running in the same (parallel) or in opposite (antiparallel) directions [48]. A regular meshing of the side chains in a coiled-coil requires that the side chains occupy equivalent positions around the helix. An α-helix has a fractional number of residues per turn (3.6), and thus regular meshing is not possible in an undistorted α-helix. However, a small left-handed twist of a regular right-handed α-helix can effectively reduce the number of residues per turn to 3.5, so that the positions of side chains will now repeat every two turns, equivalent to once every seven residues. Thus, coiled-coil proteins show a seven-residue or heptad repeat in their sequence. The seven residues in the repeat are given the letters *abcdefg* and, by

convention, residues *a* and *d* are those that provide the contacts at the helix–helix interface. In soluble proteins the residues at the *a* and *d* positions are hydrophobic residues, often Leu residues; the structure is therefore often referred to as a leucine zipper. The formation of the coiled-coil structure is largely driven by favourable hydrophobic interactions between the residues at the *a* and *d* positions.

An analysis of helix packing in membrane proteins shows that the most common packing angle between adjacent helices is close to 20° [43]. Helix packing with a crossing angle of about 20° gives a nearly parallel packing of the helices and thus maximizes the area of the interface between the helices. The packing has been described both as ridges into grooves packing of the 3–4 type [15] and as knobs-into-holes packing [49]. However, given the irregularity of the helix–helix interfaces and the range of crossing angles observed, it is not always easy to discern discrete ridges and grooves, and the knobs-into-holes packing model provides a more natural description of packing.

The potassium channel KcsA shown in Fig. 7 provides an example of coiled-coil packing of TM α-helices in a membrane protein. Pairing of Ala-29 on helix M1 with its corresponding residues on helix M2 (Leu-105 and Val-106) has the appearance of knobs-into-holes packing (Fig. 7). However, at other positions along the helix–helix interface, residues on one helix are paired with Gly residues on the other helix (Leu-36 on helix M1 with Ala-98 and Gly-99 on helix M2; Gly-43 on helix M1 with Val-91 in helix M2) allowing a relatively close approach of the two helices. This illustrates an important point. In a coiled-coil structure in a soluble protein, the side chains at positions *a* and *d* are hydrophobic to provide the hydrophobic driving force for dimer formation. In a membrane environment this is no longer so; hydrophobic interactions cannot be important in oligomerisation of TM α-helices since hydrophobic interactions are already accounted for in insertion of the helices into the lipid bilayer. It may then be better to have a small residue such as Gly at the points of contact between the helices to

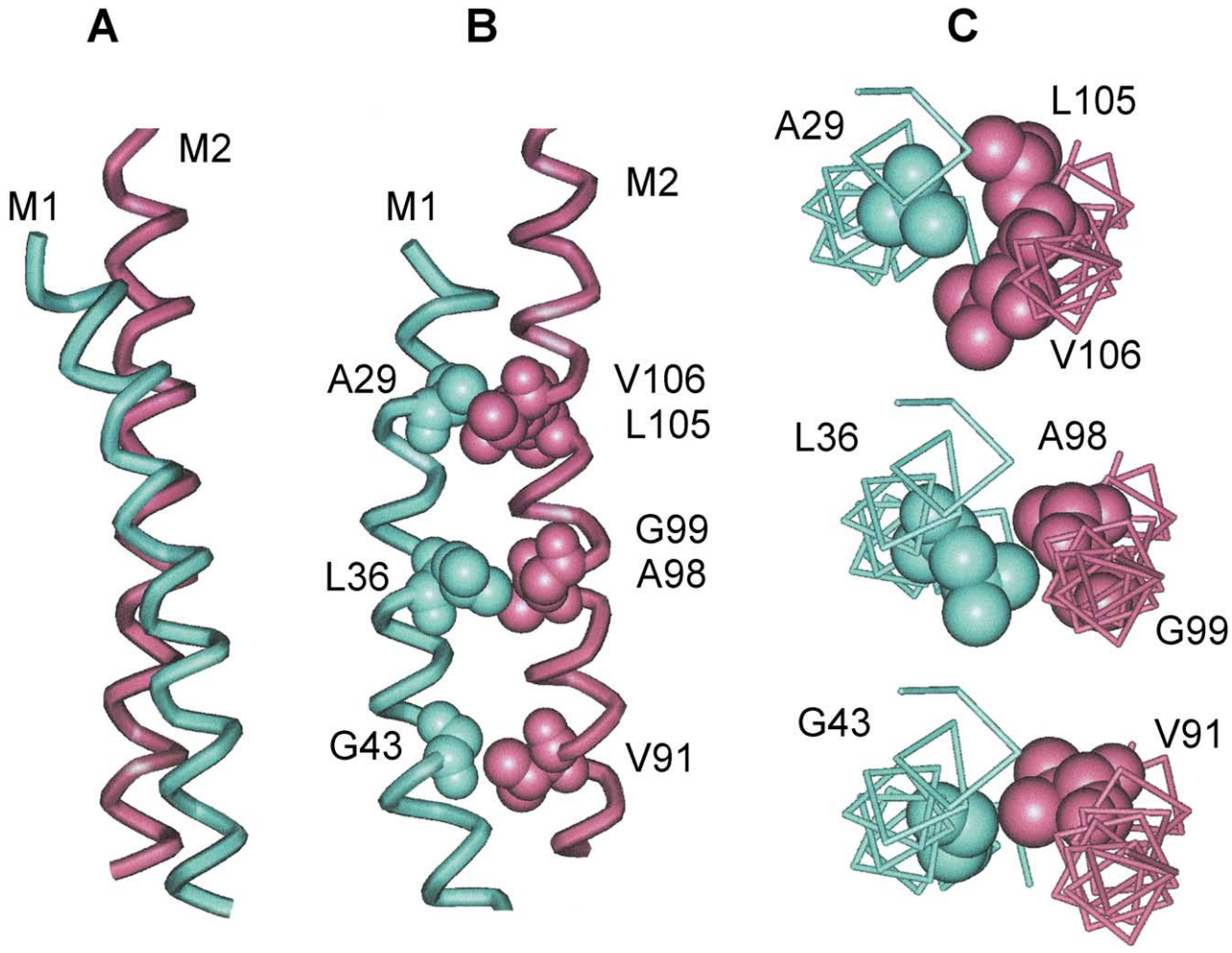

Fig. 7. Coiled-coil packing of helices M1 and M2 in the potassium channel KcsA. (A) shows the close contact between helices M1 and M2 along their length. (B) shows the heptad repeat in M1 and how residues Ala-29, Leu-36 and Gly-43 contact the corresponding residues in helix M2. (C) shows a view down the long axes of the helices, showing the nature of the packing at the sites of close contact between the helices. Ala-29 packs as knobs-into-holes but packing at the two other sites involves Gly residues, as shown.

maximize van der Waals contact between the helices rather than a hole in one helix aligned with a knob in the other. The absence of a side chain in Gly produces a flat surface against which the side chain of another residue can pack. This allows two helices to come close together, aiding close contact between the other interfacial side chains. The lack of a side chain also means that with Gly there will be no loss of side chain entropy on oligomerisation, whereas other side chains will suffer a loss of rotomeric freedom when packed at the interface. Gly is very commonly found in TM α-helices [20,50]. An analysis of a number of membrane protein crystal structures has shown that the presence of a Gly residue does not perturb the structure of a TM α-helix [51].

Packing of TM α-helices in the Ca^{2+}-ATPase is much less regular than in KcsA. It is possible that this reflects functional differences between the two types of protein. KcsA, as an ion channel, is required to be relatively rigid, acting as a simple channel once opened. The presence of surface Trp residues in KcsA could help to lock KcsA firmly into the lipid bilayer and regular packing of the TM α-helices would also help to generate a rigid structure. In contrast, the TM α-helices in the Ca^{2+}-ATPase have to undergo major conformational changes as part of the transport process (Section 5). Strong interactions between all the TM α-helices in the Ca^{2+}-ATPase would result in a high activation energy for any process requiring a change in helix packing, leading to a slow rate for transport.

Fig. 8 shows an example of two helices (M8 and M10) in the Ca^{2+}-ATPase with a packing angle of about 20°. Packing appears to be of the 3–4 class as shown in Fig. 8A and B. However, packing also fits well into the expectations of knobs-into-holes packing, with Ser-974 in M8 packing into the hole between Thr-906 and Ile-907 in M10 and Val-977 in M8 packing into the hole between Cys-9120 and Asn-911, as shown in Fig. 8C and D. This illustrates the difficulty in distinguishing between the two modes of

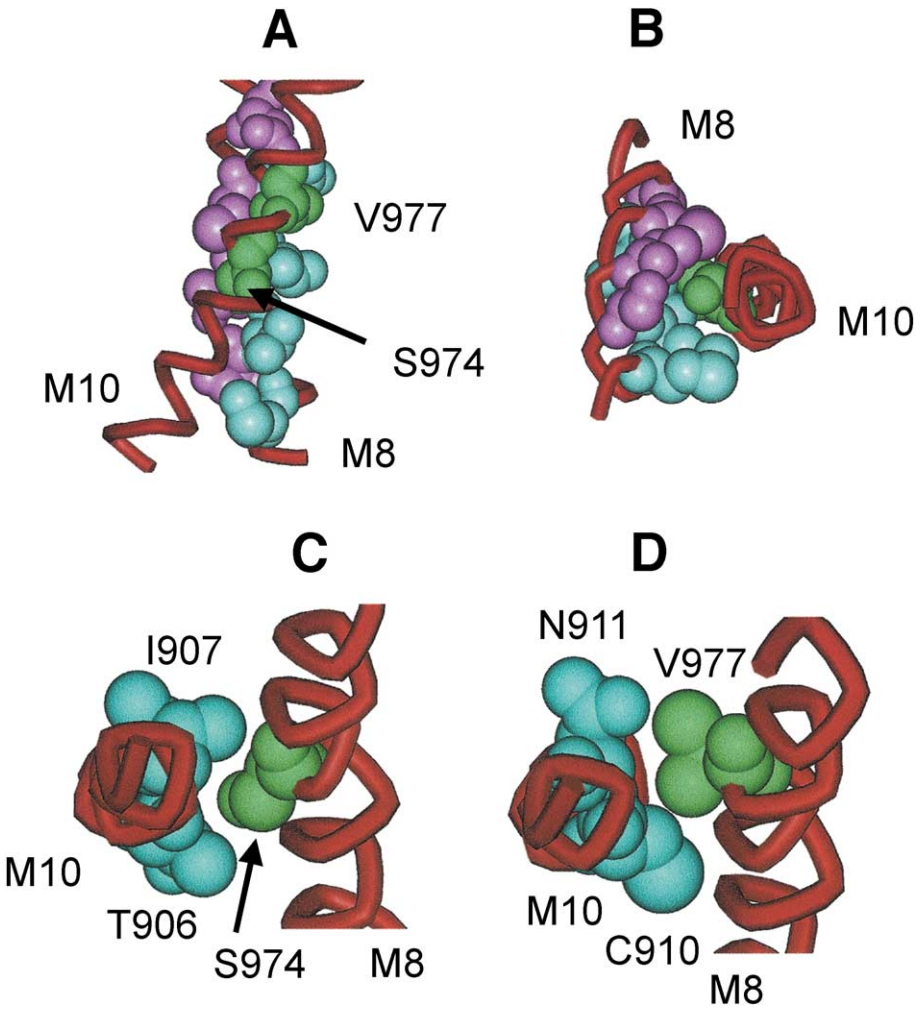

Fig. 8. Packing of helices M8 and M10 in the Ca^{2+}-ATPase in its Ca^{2+}-bound form. Packing can de described as either ridges into grooves of the 3–4 pattern (A, B) or knobs-into-holes (C, D). In A and B the ridges in helix M8 are shown in purple (Ser-902, Thr-906, Cys-910, Asn-914) and blue (Met-899, Val-903, Ile-907, Asn-911) and the ridge in M10 that packs between these two ridges is shown in green (Ser-974, Val-977). (A) shows a view normal to the bilayer surface and (B) shows a view down the long axis of helix M10. (C) and (D) show how packing of Ser-974 and Val-977 in M8 can also be described as knobs-into-holes packing. The views shown in (C) and (D) are down the long axis of helix M10.

packing when the ridges and grooves are irregular. Helix–helix packing of most of the other helices in the Ca^{2+}-ATPase is rather irregular, neighbouring helices coming into contact at just one point, often involving just one or two residues on each helix at the crossing point. The one exception is the packing of helices M5 and M7, involving Gly-770 in M5 and Gly-841 and Gly-845 in M7 (Fig. 9). The motif GxxxG in the TM α-helix of glycophorin has been shown to drive dimerisation [52,53] and the motif VVxxGAxxGI has been shown to drive dimerisation of the M13 coat protein [54]. Again, the association of the α and β chains of MHC class II to form the αβ heterodimer has been suggested to involve several Gly residues on one face of the α-helical TM domain [55]. Further, an analysis of predicted TM α-helices found that the GxxxG motif occurs more often than would have been expected by chance [56]. Although there are a number of GxxxG sequences in the Ca^{2+}-ATPase, only one occurs within the TM region, the Gly-841/Gly-845 sequence in M7. This packs against Gly-770 in M5 allowing helices M5 and M7 to cross at an angle of 20° with close packing at the crossing point (Fig. 9). Since M5 is involved in binding Ca^{2+} this close packing could be important for functioning of the Ca^{2+}-ATPase, as described in Section 5.

The free energy of association of two helices in a lipid bilayer ΔG_a can be written as:

$$\Delta G_a = \Delta G_{HH} + n/2\Delta G_{LL} - n\Delta G_{HL}$$

where ΔG_{HH}, ΔG_{LL} and ΔG_{HL} are the free energies of helix–helix, lipid–lipid and helix–lipid interactions, respectively, and it is assumed that formation of a helix–helix pair displaces n molecules of lipid from around the two helices. Dimerisation could be driven by a favourable value for ΔG_{HH}, arising, for example, from salt bridge or hydrogen bonding interactions between the two helices, although, in practice, this turns out to be rare. Good packing at the helix–helix interface with strong van der Waals interactions could also contribute to a favourable value for ΔG_{HH}. Weak interactions between the polar headgroups of the lipids and the helices and poor packing between the lipid fatty acyl chains and the rough surface of the TM α-helices would also drive dimerisation since then ΔG_{HL} will be small compared to ΔG_{HH} and ΔG_{LL}. Any decrease in motional freedom for the lipid fatty acyl chains due to the presence of the relatively rigid TM α-helix will lead to increased order for the chains and a decrease in chain entropy, also leading to an unfavourable ΔG_{HL}. The final free energy of dimerisation will be a balance between all these terms. For example, unfavourable losses of side-chain rotomer freedom and steric clashes in one part of the structure could be offset by favourable van der Waals contacts elsewhere in the dimer.

An estimate of helix–helix interaction energy within the membrane can be made from the experiments in which bacteriorhodopsin is regenerated from fragments. The efficiency of regeneration of bacteriorhodopsin was found to decrease with an increase in the lipid/protein ratio in the membrane [41,57]. Helices A and B reassembled with the fragment CDEFG with high efficiency at molar ratios of protein/lipid of 1:30 or 1:60, forming a stable lattice of trimers. However, at a molar ratio of protein/lipid of 1:300, the fragments still reassembled but to form what was apparently an abnormal conformation of the bacteriorho-

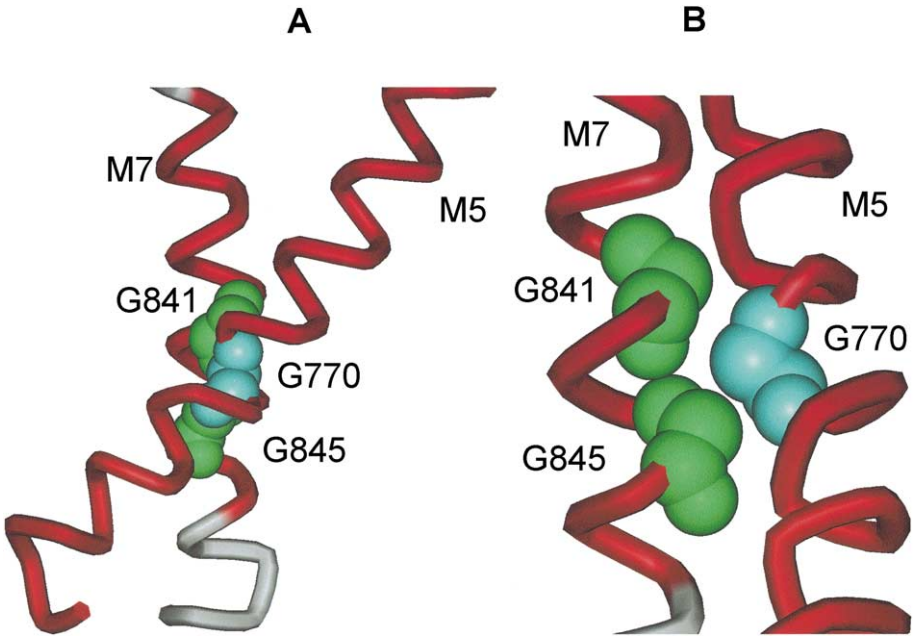

Fig. 9. Packing of helices M5 and M7 in the Ca^{2+}-ATPase in its Ca^{2+}-bound form. (A) shows that the helices pack with a crossing angle of about 20°. The view in (B) shows how Gly-770 in M5 packs closely to Gly-841 and Gly-845 in M7.

dopsin molecule. At a molar ratio of protein/lipid of 1:3000, no reassembly was observed [41,57]. A highly simplified model for the aggregation process gives an estimate for the energetics of the process [58]. For simplicity, consider a single peptide molecule (P) associating with a pre-formed six-peptide fragment (F) to give a bacteriorhodopsin molecule (B), described by an association constant K_a

$$P + F \overset{K_a}{\leftrightarrows} B.$$

With the association constant expressed in mole fraction units, 90% formation of B at a mole fraction of F of 0.017 (corresponding to a molar ratio of protein/lipid of 1:60) and a twofold excess of P would require a K_a value of about 500, corresponding to a unitary free energy of association ΔG° of about 15 kJ mol^{-1}. This estimate for the free energy of association can be compared with that that could arise from poor packing between lipid and protein, as described by White and Wimley [58]. The free energy cost of creating a cavity in the hydrophobic core of a soluble protein has been estimated to be about 125 J mol^{-1} $Å^{-3}$ [59]. The volume of a methyl group is 54 $Å^3$ so that the energy cost of creating a void equivalent to a methyl group is 6.7 kJ mol^{-1}. If therefore helix–helix packing was more efficient than helix–lipid packing by an amount equivalent to the volume of 2–3 methyl groups, the free energy change favouring helix aggregation would be about 13–20 kJ mol^{-1}, similar to the value estimated above for the peptide–bacteriorhodopsin interaction [58].

Estimates of helix–helix interaction energies can also be made from studies of model TM α-helices. Dimerisation of TM α-helical peptides in a lipid bilayer can be detected by observing the quenching of the fluorescence of a Trp-containing peptide of the type Ac-LysLysGlyLeu_mTrpLeu_nLysLysAla-amide by the corresponding peptide containing a dibromotyrosine residue instead of a Trp [60]. The free energy of dimerisation of pairs of peptides containing 16 or 22 Leu residues in di(C18:1)PC was about 8.4 kJ mol^{-1}, the value expected if helix–helix packing were more efficient than helix–lipid packing by an amount equivalent to the volume of about one methyl group. The free energy for dimer formation increased with increasing chain length by about 0.5 kJ mol^{-1} per carbon atom [60]. This shows the importance of lipid in helix–helix interactions. A comparison can be made with the entropy change corresponding to disordering of the lipid fatty acyl chains at the gel to liquid crystalline phase transition [61], which corresponds to a free energy change of ca. 2.9 kJ mol^{-1} per carbon atom. Thus, a

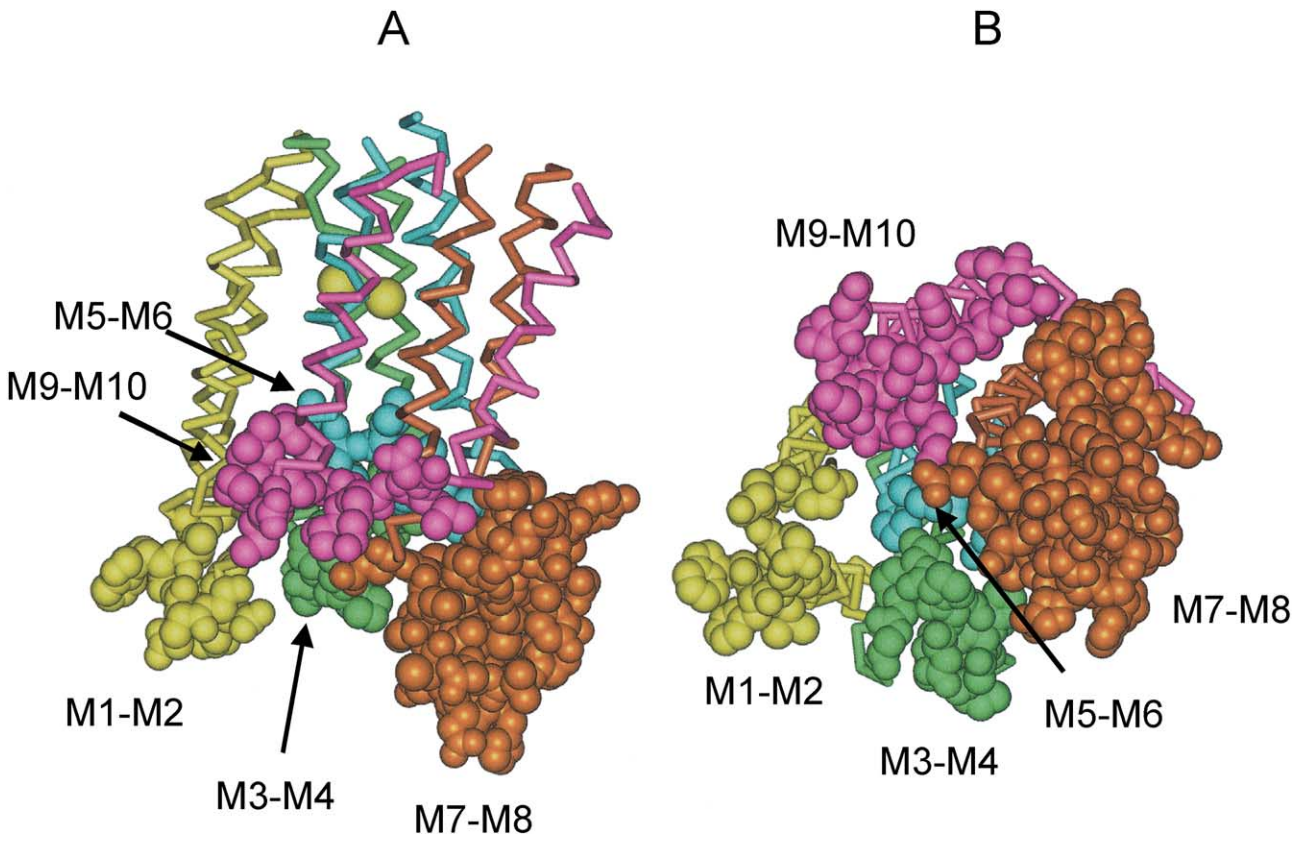

Fig. 10. Loops between TM α-helices on the lumenal side of the Ca^{2+}-ATPase in its Ca^{2+}-bound form. Loops between helices are shown in space-fill format. Helix pairs M1/M2, M3/M4, M5/M6, M7/M8 and M9/M10 are shown in yellow, green, blue, brown and purple, respectively. (A) shows a side view with the lumenal side at the bottom. (B) shows an end-on view from the lumenal side of the membrane.

relatively small increase in chain order caused by the presence of the peptide could make a significant contribution to the free energy for oligomerisation of TM α-helices.

A chain-length dependence of the energy of helix–helix packing could be part of the explanation for the chain-length dependence of the activities of some membrane proteins. For example, the ATPase activity of the Ca^{2+}-ATPase is greatest in di(C18:1)PC, with lower activities in phosphatidylcholines with shorter or longer fatty acyl chains [62]. The TM α-helices of the Ca^{2+}-ATPase are only linked by small loops on the lumenal side of the membrane, these loops making little contact with each other (Fig. 10). The small degree of contact between the lumenal loops means that, without the constraint provided by the surrounding lipid bilayers, pairs of helices would tend to move apart, destroying the structure of the TM α-helical bundle. This would have important consequences for the function of the Ca^{2+}-ATPase since transport of Ca^{2+} across the membrane must involve changes in the packing of the helices, as described. Changes in the energies of helix–helix interactions as a result of changing phospholipid chain length could therefore affect activity. The low activity of the Ca^{2+}-ATPase in gel-phase lipid with a very slow rate of phosphorylation by ATP [63] could also follow from changes in helix packing since the free energy of association of model TM α-helices is increased in gel-phase lipid [60].

5. Comparison of E1 and E2 conformations of the Ca^{2+}-ATPase

It has not yet proved possible to crystallize the Ca^{2+}-ATPase in a simple Ca^{2+}-bound form, but crystals have been obtained for the Ca^{2+}-free ATPase in the presence of an

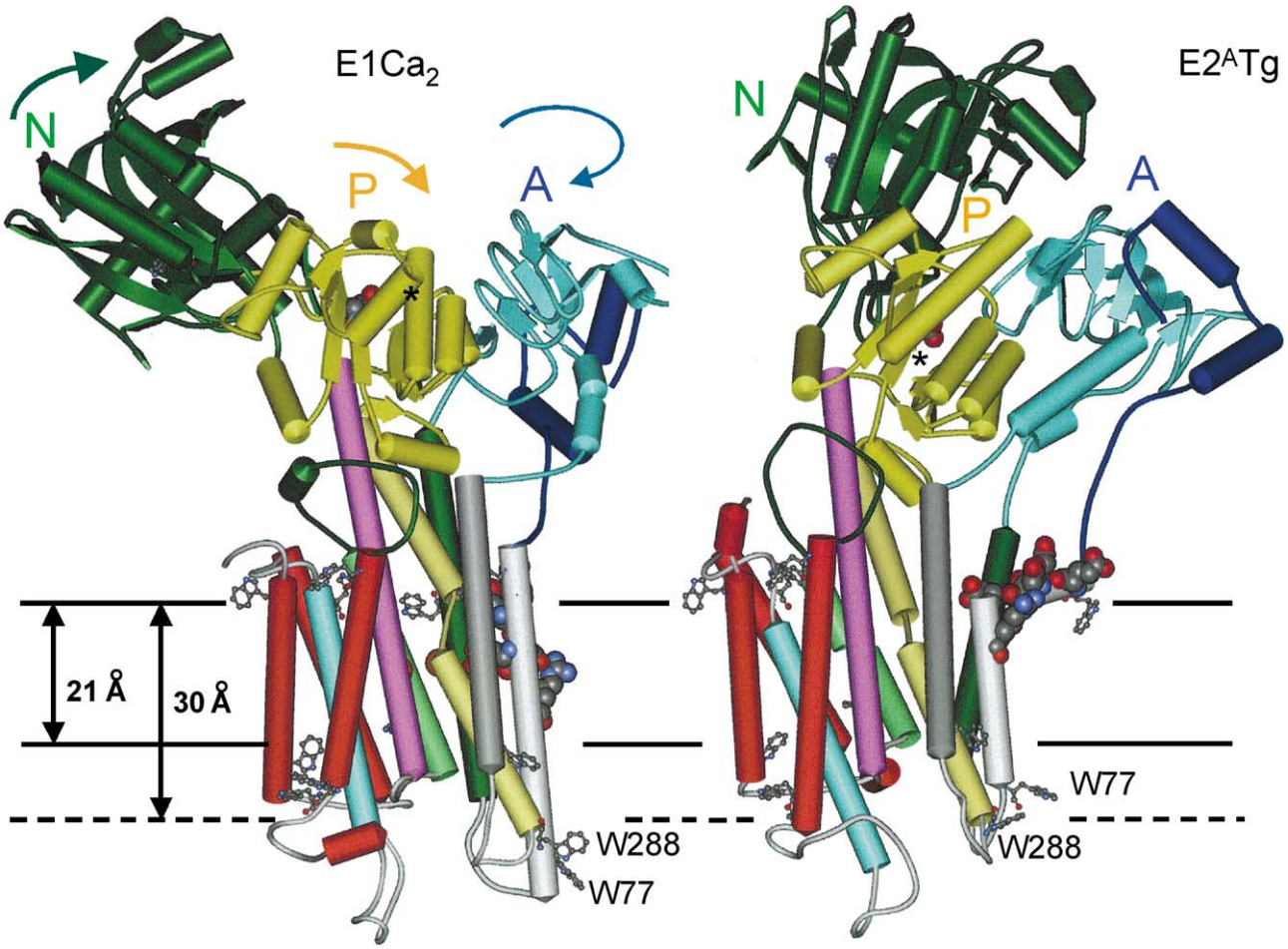

Fig. 11. Comparison of the structures of the Ca^{2+}-ATPase in its Ca^{2+}-bound ($E1Ca_2$) and Ca^{2+}-free, thapsigargin-bound ($E2^ATg$) forms. The three cytoplasmic domains A, P and N are coloured blue, yellow and green, respectively. The TM α-helices are coloured as follows: M1, light grey; M2, dark green; M3, dark grey; M4, yellow; M5, lilac; M6, light green; M7, red; M8, light blue; M9, red; M10, red. Changes in helices M7, M9 and M10 (red) are relatively minor between the $E1Ca_2$ and $E2^ATg$ conformations. Asp-351, the residue phosphorylated by ATP, is shown in space-fill representation and marked with an asterisk. Charged residues in M1 are also shown in space-fill representation. The two bound Ca^{2+}-ions in the $E1Ca_2$ structure are shown in orange. Trp residues are shown in ball-and-stick representation. Two possible positions for the lumenal side of the membrane are marked, corresponding to hydrophobic thicknesses of 21 and 30 Å for the Ca^{2+}-ATPase. The arrows show the directions of rotation of the A, P and N domains required to convert from the $E1Ca_2$ to the $E2^ATg$ conformation. (PDB files 1EUL and 1IWO).

inhibitor, thapsigargin [65]. Thapsigargin binds to the Ca^{2+}-ATPase to give a form that has the spectroscopic properties of the E2 state and, like the E2 state, does not bind Ca^{2+} from the cytoplasmic side of the membrane; unlike the normal E2 state, however, the ATPase is not phosphorylated by P_i [66]. The thapsigargin-bound state of the ATPase has therefore been described as a modified E2 state, $E2^{A}Tg$ [66]. The crystal structure of Ca^{2+}-free, thapsigargin-bound Ca^{2+}-ATPase has been determined [65] and is similar to that observed in low resolution studies for the Ca^{2+}-free, vanadate-bound ATPase, believed to be in a conformation related to that of E2P [67]. The cytoplasmic region of the ATPase in $E2^{A}Tg$ is much more compact than that in $E1Ca_2$ (Fig. 11). In the transformation from $E1Ca_2$ to $E2^{A}Tg$, the nucleotide binding domain rotates by almost 90° to adopt an almost vertical orientation. In part this is made possible by a smaller rotation of the phosphorylation domain, which undergoes about a 30° rotation with respect to the membrane. Finally,

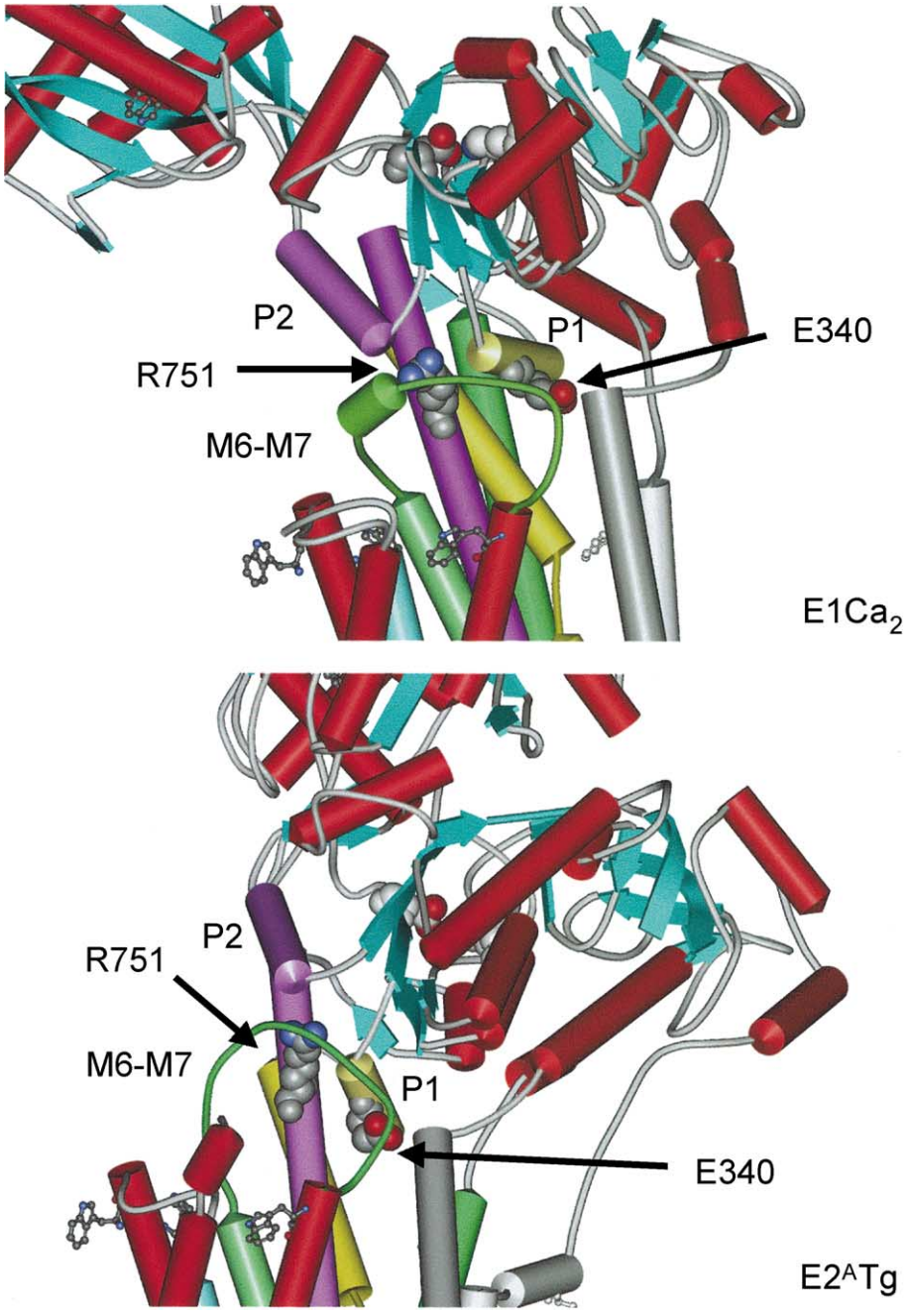

Fig. 12. Comparison of the structures of the P domain of the Ca^{2+}-ATPase in the $E1Ca_2$ and $E2^{A}Tg$ conformations. The colour code for the TM α-helices is as in Fig. 11. The cytoplasmic helices P1 and P2 are coloured yellow and purple, respectively. Glu-340 that hydrogen bonds between P1 and TM α-helix M3, and Arg-751 that hydrogen bonds between TM α-helix M5 and P2 are shown in space-fill representation.

the A domain rotates about 110° horizontally. Despite the large movement of the phosphorylation and nucleotide binding domains, their structures hardly change [65].

The change in orientation of the phosphorylation domain is directly related to tilting of the TM α-helices [65]. These changes are complex; movement of any one element of the structure requires movement of several others, for steric reasons. What is clear is that changes in the phosphorylation domain are linked to, and require, changes in the TM region (Fig. 12). Changes in helices M7–M10 are relatively small, but there are major changes for the other helices. The changes in M1 are particularly complex. In the Ca^{2+}-bound form, charged residues Glu-51 and Glu-55 are located at the top of the helix, Glu-58 facing in towards the Ca^{2+} ion at site II with Asp-59 and Arg-63 forming an ion pair exposed to the lipid bilayer (Figs. 1 and 11). In $E2^{A}Tg$ these residues have moved upwards with a bend at Asp-59 to form an amphipathic helix with hydrophobic residues on one side and Glu-58 and Asp-59 on the other, and Arg-63 now snorkels up to the lipid–water interface (Fig. 11). The bottom of helix M1 is defined in $E2^{A}Tg$ by Trp-77 and by Glu-79. As shown in Fig. 11, Trp-77 and Glu-79 move upwards in $E2^{A}Tg$ compared to $E1Ca_2$ as a result of the upward movement of the whole helix. M5 tilts about a pivoting point at about Glu-770 [65]. As shown in Fig. 9, M5 packs tightly with M7 at this point. M2 moves to a more upright conformation in $E2^{A}Tg$ (Fig. 11).

These changes in helix tilt are connected to changes in the phosphorylation domain (Fig. 12). It has been suggested that movement of cytoplasmic helices P1 and P2 in the phosphorylation domain relative to the M6–M7 loop is important in connecting changes in the phosphorylation domain to changes in the TM helices and vice versa [5]. As shown in Fig. 12, the relationship between P1 and the M6–M7 loop is very different in the $E1Ca_2$ and $E2^{A}Tg$ structures. Helix P1 is connected to the top of M3 by a hydrogen bond to Glu-340 and M5 is connected to the M6–M7 loop by Arg-751. Movements in the phosphorylation domain will therefore be linked to movements in TM helices M3 and M5. In $E1Ca_2$ the top of M2 is linked to M4 by a hydrogen bond to Arg-324; in $E2^{A}Tg$ M4 moves, resulting in a movement of M2.

Changes in the packing of the TM α-helices result in changes at the Ca^{2+}-binding sites [65]. The backbones of residues Glu-771 and Glu-908 hardly move between the Ca^{2+}-bound and Ca^{2+}-free structures (Fig. 13). However, in the absence of Ca^{2+}, Thr-799 and Asn-768 at site I reorient and Asp-800, which in the presence of Ca^{2+} bridges between the two binding sites, moves away. At site II, Val-304, Asn-796 move away on loss of Ca^{2+} and Glu-309 reorients to point away from the site. Further, Glu-58 from M1, which in $E1Ca_2$ points towards site II, is located well away from the site in $E2^{A}Tg$. Of the two sites, site I appears to be more intact in the Ca^{2+}-free form than site II, with Glu-908 and Glu-771 only changing slightly in position, and Asp-800 being located more at site I in the Ca^{2+}-free form than in the Ca^{2+}-bound form, whereas at site II Asp-800 and Glu-309 have both moved away (Fig. 13). Ca^{2+} binding to the ATPase is cooperative, with Ca^{2+} ions binding first to site I then to site II [5]. It was suggested that in the process of binding Ca^{2+}, Ca^{2+} ions pass through site II to reach site I, and that this would only be possible if site II were not properly formed in the absence of Ca^{2+} at site I; it was also suggested that access to site II in the Ca^{2+}-bound form was blocked by Glu-309 and that Glu-309 would have to relocate to allow Ca^{2+} ions access to sites I and II [5]. These ideas are consistent with the structures shown in Fig. 13. Comparison of the Ca^{2+}-free and Ca^{2+}-bound structures suggests that a single binding site for Ca^{2+} could exist in the Ca^{2+}-free structure in the vicinity of Glu-908 and Glu-771. Binding of Ca^{2+} in this region would restructure the region to form site I, relocation of Asp-800

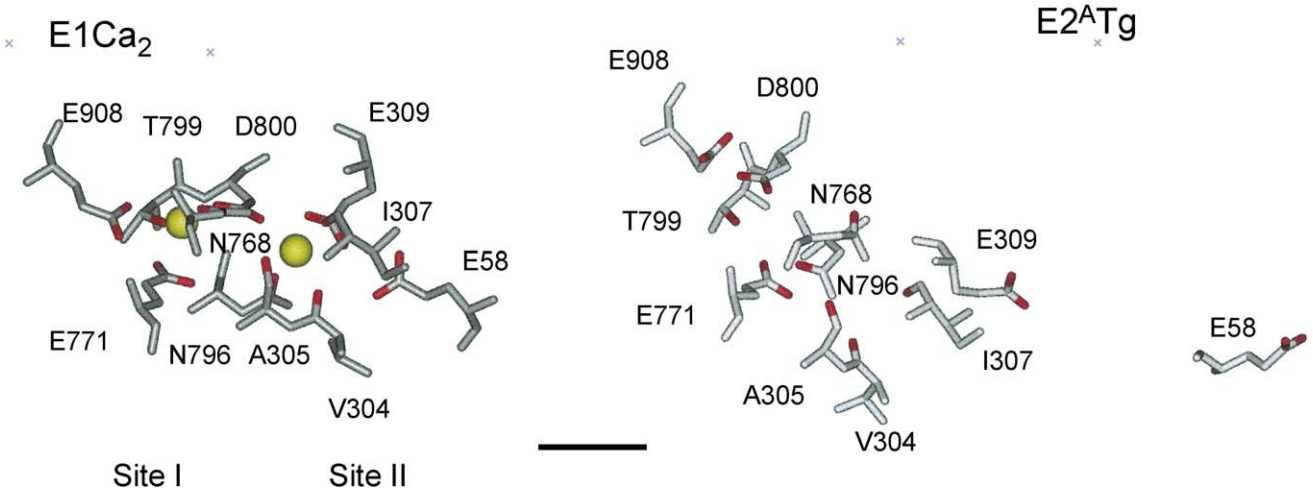

Fig. 13. Comparison of the Ca^{2+} binding regions in the $E1Ca_2$ and $E2^{A}Tg$ conformations of the Ca^{2+}-ATPase. Ligands important in binding Ca^{2+} ions at sites I and II in the $E1Ca_2$ conformation are shown, together with the positions of these same residues in the $E2^{A}Tg$ conformation. The bar represents 10 Å.

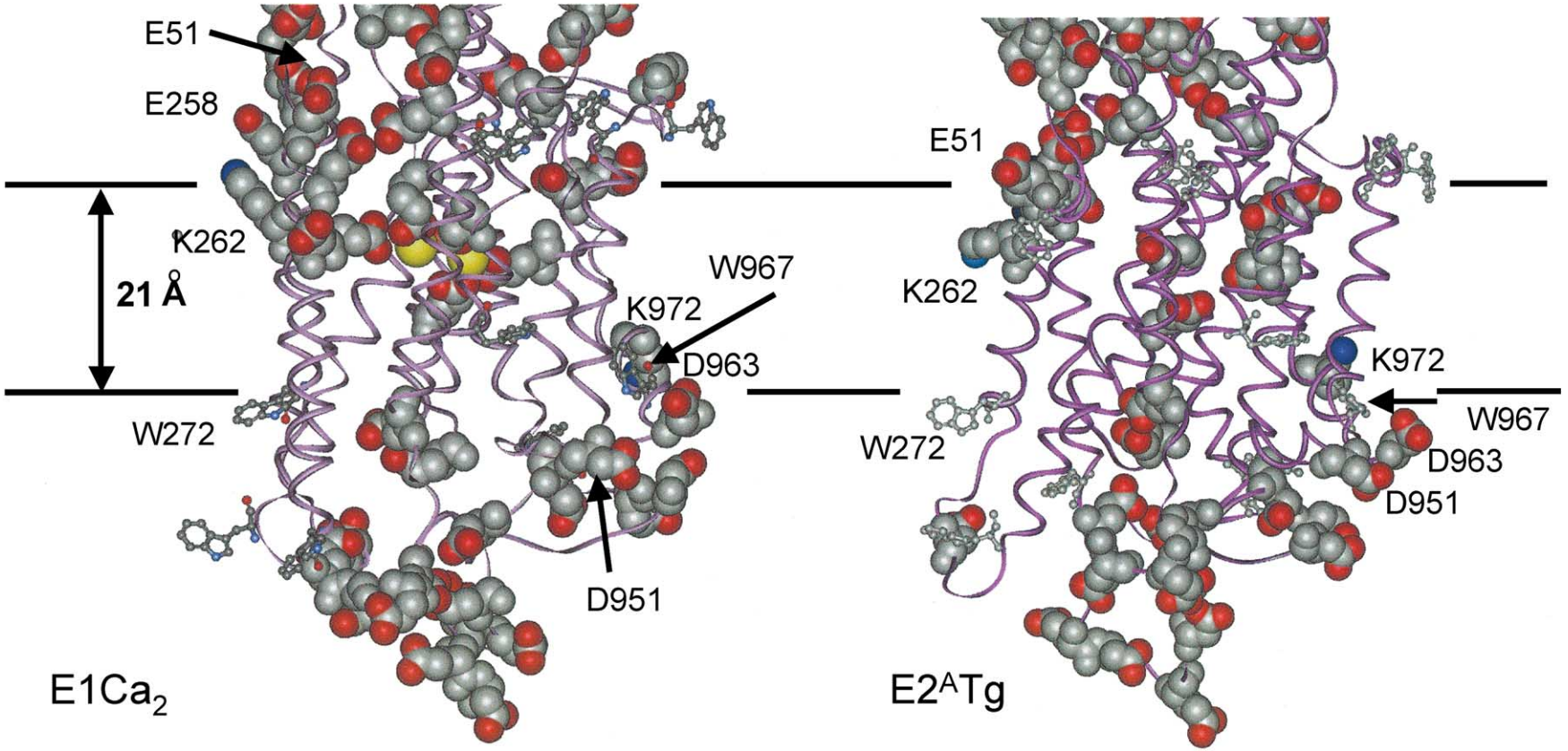

Fig. 14. Acidic residues in the TM region of the Ca^{2+}-ATPase and close to the cytoplasmic and lumenal surfaces, in the $E1Ca_2$ and $E2^{A}Tg$ conformations. Acidic residues are shown in space-fill representation and Trp residues are shown in ball-and-stick representation. Also shown are two Lys residues, Lys-262 and Lys-972, that help to define the probable locations of the cytoplasmic and lumenal surfaces of the membrane, 21 Å apart.

helping to form site II. Movement of Glu-309 and Glu-58 following binding of the second Ca^{2+} ion would complete site II. Movement of Glu-58 between the Ca^{2+}-free and Ca^{2+}-bound structures is particularly marked (Fig. 13). It was suggested that helix M1 and Glu-58 could be important in both the access pathway to the Ca^{2+} binding sites and in the gating process in which the Ca^{2+} binding sites are closed after Ca^{2+} ions have bound [5]. It was noted that in $E1Ca_2$ a short channel lined by Glu-58 in M1 leads between Glu-109 and Glu-55 to site II, providing a possible entry pathway for the Ca^{2+} ions [5]. In the $E2^{A}Tg$ form this channel is of wider diameter and is water-filled [65], strengthening the suggestion that it could be an important part of the access pathway to the Ca^{2+} binding sites.

In the alternating site model for the Ca^{2+}-ATPase, a single pair of Ca^{2+}-binding sites changes from being exposed to the cytoplasm in E1 to being exposed to the lumen in the E2 conformation [3]. This model suggests that a clear pathway ought to be visible in the structure of the $E2^{A}Tg$ form of the ATPase. In fact, as shown in Figs. 11 and 14, no such clear pathway is visible. One explanation for this could be that the $E2^{A}Tg$ conformation is an abnormal conformation for the

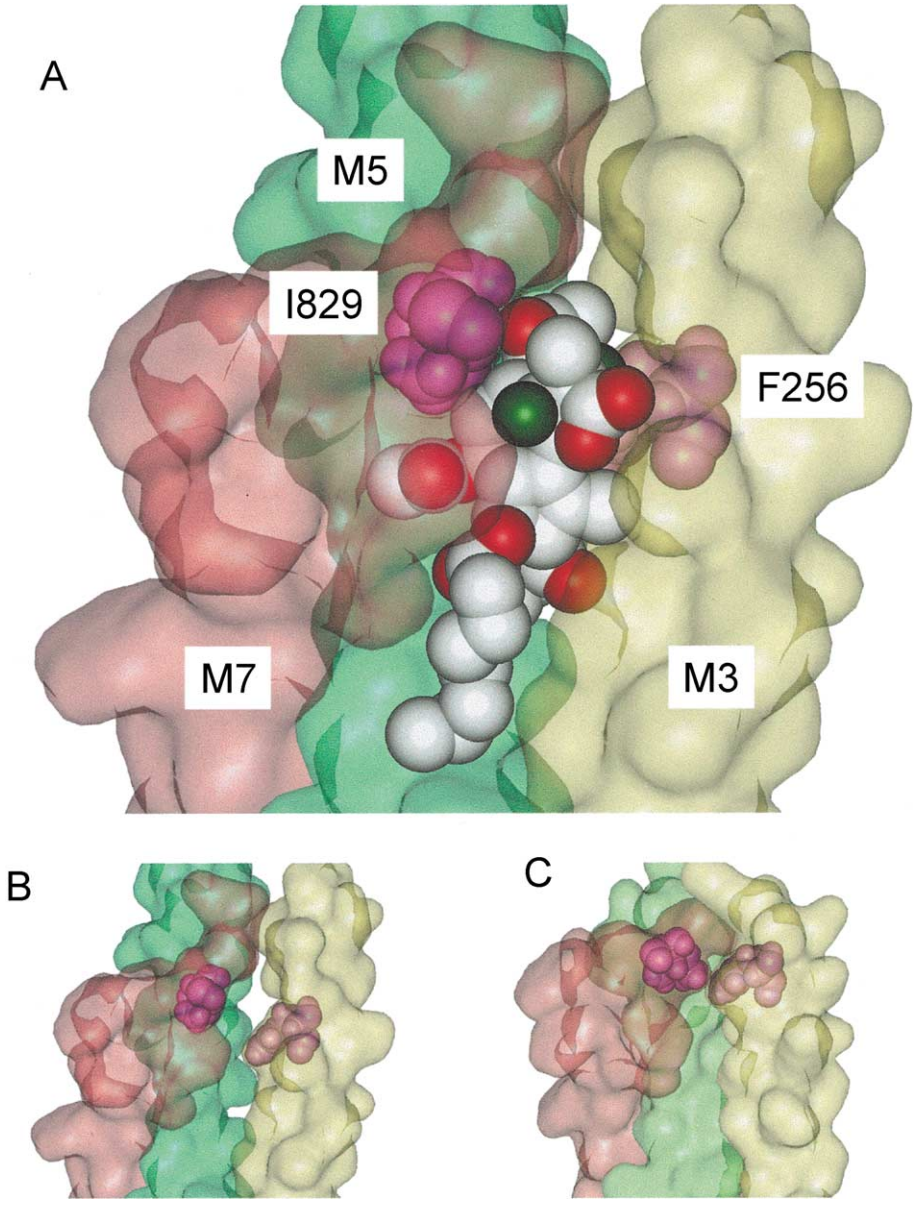

Fig. 15. The binding site for thapsigargin on the Ca^{2+}-ATPase. For simplicity, only helices M3 (yellow), M5 (green) and M7 (brown) are shown in surface format. (A) The bound thapsigargin molecule is shown in space-fill representation as are residues Phe-256 and Ile-829, important in binding the inhibitor. The two key -OH groups, at C7 and C11 of the thapsigargin molecule, are shown in dark green. (B) shows the same region as in (A) but with the thapsigargin molecule removed. (C) shows the region around Phe-256 and Ile-829 in the $E1Ca_2$ structure.

ATPase, and that a clear lumenal release pathway would have been visible in a 'normal' E2 conformation. The alternative explanation is, of course, that the alternating site model is incorrect. Indeed, evidence has been presented elsewhere for an alternating four-site model (Fig. 2) in which no pathway would be expected from the pair of Ca^{2+} transport sites to the lumenal side of the membrane in the E2 conformation [5].

The binding site for thapsigargin on the Ca^{2+}-ATPase is illustrated in Fig. 15. Thapsigargin binds in a cleft between helices M3, M5 and M7. The polar end of the thapsigargin molecule is located between Phe-256 and Ile-829, close to the expected position of the glycerol backbone region of the surrounding lipid bilayer. Experiments using site-directed mutagenesis had identified Phe-256 as a key residue in binding thapsigargin [68]. Residues Ser-261, Ser-265, Cys-268 and Trp-272 in M3, shown not to be important in binding thapsigargin [71], are located on the face of M3 pointing away from the binding site for thapsigargin. Residues Phe-835 and Tyr-837 in M7, also shown not to be important in binding thapsigargin [71], also point away from the binding site. Phe-834 on M7 does point towards the binding site, but replacement of Phe by a smaller Ala residue would not be expected to affect binding of thapsigargin, as observed experimentally [71].

The alkyl chain of the thapsigargin molecule lies along the hydrophobic surface of helix M5. The two –OH groups in thapsigargin, at positions C7 and C11, have been shown to be essential for activity [69]. These will help locate the thapsigargin molecule in its binding site and also, presumably, help determine the conformation of the molecule in the key region inserted between Phe-256 and Ile-829. In the structure of the Ca^{2+}-bound ATPase, the space between Phe-256 and Ile-829 is much narrower than in the Ca^{2+}-free form (Fig. 15). By keeping TM α-helices M3 and M7 apart, thapsigargin presumably prevents the ATPase from adopting a conformation in which it can bind Ca^{2+} ions and be active. Thus, inhibition by thapsigargin is indirect and based on steric factors. A variety other clefts exist on the surface of the ATPase between TM α-helices, including that between helices M2 and M9 to which phospholamban binds (Fig. 5). Other hydrophobic inhibitors of the Ca^{2+}-ATPase such as *t*-butyl hydroquinone (BHQ), nonyl phenol and curcumin [70] could bind in these clefts. A variety of other hydrophobic molecules, including cholesterol and simple alkanes, have been suggested to bind to 'non-annular' sites on the Ca^{2+}-ATPase, stimulating activity for the Ca^{2+}-ATPase reconstituted into di(C14:1)PC [27,29,33]. These non-annular sites could also be located in clefts between the TM α-helices [27,29,33].

Acknowledgements

I thank the BBSRC for financial support for the unpublished work included in this review.

References

[1] C. Toyoshima, M. Nakasako, H. Nomura, H. Ogawa, Nature 405 (2000) 647–655.
[2] J.V. Moller, B. Juul, M. le Maire, Biochim. Biophys. Acta 1286 (1996) 1–51.
[3] L. de Meis, The Sarcoplasmic Reticulum, Wiley, New York, 1981.
[4] W.P. Jencks, T. Yang, D. Peisach, J. Myung, Biochemistry 32 (1993) 7030–7034.
[5] A.G. Lee, J.M. East, Biochem. J. 356 (2001) 665–683.
[6] A.G. Lee, Biochim. Biophys. Acta 1376 (1998) 381–390.
[7] M.C. Wiener, S.H. White, Biophys. J. 61 (1992) 434–447.
[8] H. Michel, J. Deisenhofer, Curr. Top. Membr. Transp. 36 (1990) 53–69.
[9] U. Ermler, H. Michel, M. Schiffer, J. Bioenerg. Biomembranes 26 (1994) 5–15.
[10] M. Roth, A. Lewit-Bentley, H. Michel, J. Deisenhofer, R. Huber, D. Oesterhelt, Nature 340 (1989) 659–662.
[11] M. Roth, B. Arnoux, F. Reiss-Husson, Biochemistry 30 (1991) 9403–9413.
[12] W.C. Wimley, S.H. White, Nat. Struct. Biol. 3 (1996) 842–848.
[13] W.M. Yau, W.C. Wimley, K. Gawrisch, S.H. White, Biochemistry 37 (1998) 14713–14718.
[14] D.A. Doyle, J.M. Cabral, R.A. Pfuetzner, A. Kuo, J.M. Gulbis, S.L. Cohen, B.T. Chait, R. Mackinnon, Science 280 (1998) 69–77.
[15] D.C. Rees, A.J. Chirino, K.H. Kim, H. Komiya, in: S.H. White (Ed.), Membrane Protein Structure, OUP, New York, 1994, pp. 3–26.
[16] D.M. Engelman, T.A. Steitz, A. Goldman, Annu. Rev. Biophys. Biophys. Chem. 15 (1986) 321–353.
[17] J.M. East, A.G. Lee, Biochemistry 21 (1982) 4144–4151.
[18] A.P. Starling, Y.M. Khan, J.M. East, A.G. Lee, Biochem. J. 304 (1994) 569–575.
[19] A.P. Starling, J.M. East, A.G. Lee, Biochemistry 32 (1993) 1593–1600.
[20] C. Landolt-Marticorena, K.A. Williams, C.M. Deber, R.A.F. Reithmeier, J. Mol. Biol. 229 (1993) 602–608.
[21] E. Wallin, T. Tsukihara, S. Yoshikawa, G. von Heijne, A. Elofsson, Protein Sci. 6 (1997) 808–815.
[22] D.C. Rees, L. DeAntonio, D. Eisenberg, Science 245 (1989) 510–513.
[23] D.T. Jones, W.R. Taylor, J.M. Thornton, FEBS Lett. 339 (1994) 269–275.
[24] D. Donnelly, J.P. Overington, S.V. Ruffle, J.H.A. Nugent, T.L. Blundell, Protein Sci. 2 (1993) 55–70.
[25] J.M. East, D. Melville, A.G. Lee, Biochemistry 24 (1985) 2615–2623.
[26] R.J. Froud, J.M. East, E.K. Rooney, A.G. Lee, Biochemistry 25 (1986) 7535–7544.
[27] A.C. Simmonds, J.M. East, O.T. Jones, E.K. Rooney, J. McWhirter, A.G. Lee, Biochim. Biophys. Acta 693 (1982) 398–406.
[28] A.C. Simmonds, E.K. Rooney, A.G. Lee, Biochemistry 23 (1984) 1432–1441.
[29] J. Ding, A.P. Starling, J.M. East, A.G. Lee, Biochemistry 33 (1994) 4974–4979.
[30] R.J. Froud, C.R.A. Earl, J.M. East, A.G. Lee, Biochim. Biophys. Acta 860 (1986) 354–360.
[31] R.J. Webb, J.M. East, R.P. Sharma, A.G. Lee, Biochemistry 37 (1998) 673–679.
[32] S. Mall, R. Broadbridge, R.P. Sharma, A.G. Lee, J.M. East, Biochemistry 39 (2000) 2071–2078.
[33] A.G. Lee, J.M. East, P. Balgavy, Pestic. Sci. 32 (1991) 317–327.
[34] T. Toyofuku, K. Kurzydlowski, M. Tada, D.H. MacLennan, J. Biol. Chem. 269 (1994) 22929–22932.
[35] A.M. Mata, I. Matthews, R.E.A. Tunwell, R.P. Sharma, A.G. Lee, J.M. East, Biochem. J. 286 (1992) 567–580.
[36] M. Asahi, Y. Kimura, R. Kurzydlowski, M. Tada, D.H. MacLennan, J. Biol. Chem. 274 (1999) 32855–32862.
[37] J.L. Popot, C. de Vitry, A. Atteia, in: S.H. White (Ed.), Membrane Protein Structure, OUP, New York, 1994, pp. 41–96.
[38] M.J. Liao, E. London, H.G. Khorana, J. Biol. Chem. 258 (1983) 9949.

[39] J.L. Popot, S.E. Gerchman, D.M. Engelman, J. Mol. Biol. 198 (1987) 655–676.
[40] F.A. Samatey, G. Zaccai, D.M. Engelman, C. Etchebest, J.L. Popot, J. Mol. Biol. 236 (1994) 1093–1104.
[41] T.W. Kahn, D.M. Engelman, Biochemistry 31 (1992) 6144–6151.
[42] T. Marti, J. Biol. Chem. 273 (1998) 9312–9322.
[43] J.U. Bowie, J. Mol. Biol. 272 (1997) 780–789.
[44] D.C. Rees, H. Komiya, T.O. Yeates, J.P. Allen, G. Feher, Ann. Rev. Biochem. 58 (1989) 607–633.
[45] V. Chothia, M. Levitt, D. Richardson, J. Mol. Biol. 145 (1981) 215–250.
[46] C. Branden, J. Tooze, Introduction to Protein Structure, Garland Publishing, New York, 1991.
[47] F.H.C. Crick, Acta Crystallogr. 6 (1953) 689–697.
[48] A. Lupas, Trends Biochem. Sci. 21 (1996) 375–382.
[49] D. Langosch, J. Heringa, Protein Struct. Funct. Genet. 31 (1998) 150–159.
[50] M. Eilers, S.C. Shekar, T. Shieh, S.O. Smith, P.J. Fleming, Proc. Natl. Acad. Sci. U. S. A. 97 (2000) 5796–5801.
[51] M.M. Javadpour, M. Eilers, M. Groesbeek, S.O. Smith, Biophys. J. 77 (1999) 1609–1618.
[52] M.A. Lemmon, H.R. Treutlein, P.D. Adams, A.T. Brunger, D.M. Engelman, Nat. Struct. Biol. 1 (1994) 157–163.
[53] B. Brosig, D. Langosch, Protein Sci. 7 (1998) 1052–1056.
[54] K.A. Williams, M. Glibowicka, Z. Li, H. Li, A.R. Khan, Y.M.Y. Chen, J. Wang, D.A. Marvin, C.M. Deber, J. Mol. Biol. 252 (1995) 6–14.
[55] P. Cosson, J.S. Bonifacino, Science 258 (1992) 659–662.
[56] A. Senes, M. Gerstein, D.M. Engelman, J. Mol. Biol. 296 (2000) 921–936.
[57] T.W. Kahn, J.M. Sturtevant, D.M. Engelman, Biochemistry 31 (1992) 8829–8839.
[58] S.H. White, W.C. Wimley, Annu. Rev. Biophys. Biomol. Struct. 28 (2000) 319–365.
[59] A.E. Eriksson, W.A. Baase, X.J. Zhang, D.W. Heinz, M. Blaber, E.P. Baldwin, B.W. Matthews, Science 255 (1992) 178–183.
[60] S. Mall, R. Broadbridge, R.P. Sharma, J.M. East, A.G. Lee, Biochemistry 40 (2001) 12379–12386.
[61] D. Marsh, CRC Handbook of Lipid Bilayers, CRC Press, Boca Raton, 1990.
[62] A.G. Lee, Biochim. Biophys. Acta 1376 (1998) 381–390.
[63] A.P. Starling, J.M. East, A.G. Lee, Biochemistry 34 (1995) 3084–3091.
[64] D.H. MacLennan, W.J. Rice, N.M. Green, J. Biol. Chem. 272 (1997) 28815–28818.
[65] C. Toyoshima, H. Nomura, Nature 418 (2002) 605–611.
[66] M. Wictome, Y.M. Khan, J.M. East, A.G. Lee, Biochem. J. 310 (1995) 859–868.
[67] C. Xu, W.J. Rice, W. He, D.L. Stokes, J. Mol. Biol. 316 (2002) 201–211.
[68] M. Yu, L. Zhang, A.K. Rishi, M. Khadeer, G. Inesi, A. Hussain, J. Biol. Chem. 273 (1998) 3542–3546.
[69] M. Wictome, M. Holub, J.M. East, A.G. Lee, Biochem. Biophys. Res. Comm. 199 (1994) 916–921.
[70] M.J. Logan-Smith, J.M. East, A.G. Lee, Biochemistry 41 (2002) 2869–2875.
[71] P. Adams, J.M. East, A.G. Lee, C.D. O'Connor, Biochem. J. 335 (1998) 131–138.